

FG SAGITTAE: A NEWBORN R CORONAE BOREALIS STAR?¹

GUILLERMO GONZALEZ²

Astronomy Department, University of Washington, P.O. Box 351580, Seattle, WA 98195-1580

DAVID L. LAMBERT²

Department of Astronomy, University of Texas, Austin, TX 78712-1083; dll@astro.as.utexas.edu

GEORGE WALLERSTEIN

Astronomy Department, University of Washington, P.O. Box 351580, Seattle, WA 98195-1580; wall@astro.washington.edu

N. KAMESWARA RAO

Indian Institute of Astrophysics, Bangalore, 560 034 India; giridhar@iiap.ernet.in

VERNE V. SMITH

Department of Physics, University of Texas at El Paso, 500 West University, El Paso, TX 79968-0515; verne@balmer.physics.utep.edu

AND

JAMES K. MCCARTHY³

Caltech, Department of Astronomy, MS 105-24, Pasadena, CA 91125; jkm@deimos.caltech.edu

Received 1997 May 14; accepted 1997 July 18

ABSTRACT

We have monitored FG Sge's spectroscopic changes since the time just prior to its dramatic fading in 1992 August. The most significant qualitative changes in the spectrum include large variations in the strength of the C₂ molecular bands and the gradual appearance of broad blueshifted high-velocity (~ 200 km s⁻¹ relative to the photosphere) absorption components of the Na I D lines. During the deep minima of 1994 May and 1996 June, an emission-line spectrum temporarily appeared superimposed on a weak continuum; in addition to the previously reported nebular emission lines, the spectra displayed the C₂ and rare earth element lines in emission. Much of the behavior exhibited by FG Sge since 1992 resembles that seen in R CrB stars, including the photometric behavior, the evolution of the Na I D line profiles, variations of the C₂ band strengths, and the appearance of narrow emission lines.

The results of our abundance analysis (using model atmospheres with a solar He/H ratio) indicate that the carbon abundance is currently greater than that determined by Langer et al., who reported on the dramatic increase in the abundances of the rare earth elements in FG Sge. We derive higher relative abundances of the rare earths ([Me/Fe] ~ 3) than either Langer et al. or Kipper & Kipper, which we attribute to some enhancement of these elements since ~ 1970 . We confirm previous claims that the relative scandium abundance is high ([Sc/Fe] ~ 1) in FG Sge and suggest that it is the result of neutron captures by the light elements leading up to ⁴⁵Sc.

The H α profile of FG Sge is very similar to that of V854 Cen, a R CrB star deficient in H by 2–3 dex. This is the first evidence pointing toward H-deficiency in the atmosphere of FG Sge, which further strengthens its link with the R CrB class. Additional study is required before we can say definitively whether or not its atmosphere is H deficient.

Subject headings: stars: abundances — stars: AGB and post-AGB — stars: chemically peculiar — stars: individual (FG Sagittae)

1. INTRODUCTION

Over the last century, FG Sge has been a star of slowly increasing visual brightness, beginning at $m_{\text{pg}} = 13.6$ in 1894 and reaching $B = 9.6$ in 1965 (Herbig & Boyarchuk 1968; hereafter HB). The spectral type also changed dramatically: from B5 Ia in 1955, to A5 Ia in 1967 (HB), and to G2 Ia in the mid-1970s (Smolinski, Climenhaga, & Kipper 1976). Since that time the brightness has remained approximately constant, and the spectral type has remained near

F6 (Montesinos et al. 1990; Kipper & Kipper 1989). Wentzel & Fürtig (1967) pointed out that while the visual brightness had increased, the bolometric magnitude had not changed, defining a horizontal path in the temperature-luminosity plane. HB first suggested that FG Sge is the central star of an old planetary nebula, a slowly fading fossil of previous excitation when the star had a much higher temperature ($\sim 65,000$ K; Harrington & Marioni 1976)—see also Faulkner & Bessell (1970) and Flannery & Herbig (1973). Arkipova (1996) has shown that the radial velocity variations of FG Sge's photosphere are in phase with its low-amplitude light variations. Hence, FG Sge appears to be a single star that exhibits pulsation.

Remarkable changes in FG Sge's chemical composition have also occurred. In the 1960s, it had approximately solar abundances, but in the early 1970s lines of rare earth elements appeared suddenly and strengthened dramatically (Langer, Kraft, & Anderson 1974). The probable explanation for this behavior rests on the occurrence of a He-

¹ Based in part on observations collected at the Kitt Peak National Observatory, National Optical Astronomy Observatories (NOAO), which is operated by the Association of Universities for Research in Astronomy Inc. (AURA) under cooperative agreement with the National Science Foundation.

² Visiting Astronomer, Cerro Tololo Inter-American Observatory, NOAO, operated by AURA.

³ Visiting Astronomer, W. M. Keck Observatory, jointly operated by the California Institute of Technology and the University of California.

burning shell flash, which coincided with the start of the visual brightening about 100 years ago (Paczynski 1971; Schönberner 1979; Iben 1984): the star's photosphere expanded, followed by the dredge-up of s-process elements in about 1970.

In 1992 FG Sge underwent dramatic photometric variations not previously seen in this star. Its visual brightness declined suddenly by about 5 mag (Arhipova 1994), and IR observations indicated the formation of a dusty shell (Woodward et al. 1993); hence, the visual brightness decline appears to be due to dust condensation. As pointed out by Jurcsik (1993), this behavior is similar to the R CrB phenomenon. Since 1992, the star has experienced several additional fadings of varying depths. We may be witnessing, perhaps for the first time, the apparent birth of a new R CrB star. In order to address the link between FG Sge and the R CrB stars, we monitored FG Sge between 1992 and 1996, including the deep visual brightness minima of 1994 May and 1996 June, using high-resolution spectroscopy. We also report on an abundance analysis using one of our best spectra in order to constrain better the relative abundance pattern in the photosphere of FG Sge and to look for evidence of abundance changes since Langer et al.'s study.

2. OBSERVATIONS

We have obtained spectra of FG Sge with four telescopes over a period of 54 months: the Sandiford Cassegrain echelle spectrograph (McCarthy et al. 1993) was used with the 2.1 m telescope at McDonald Observatory, the echelle long focal length camera was used both with the 4 m telescopes at CTIO and KPNO, and the HIRES echelle spectrograph (Vogt et al. 1994) was used with the Keck 10 m telescope. The details of the observations are listed in Table 1, and the epoch of each spectrum is shown in Figure 1. Typical exposure times were 30-60 minutes with the 2.1 m telescope, 10-20 minutes with the 4 m telescope, and 30 minutes with the Keck telescope. Due to the large brightness fluctuations of FG Sge during the observing period, the resultant S/N varies considerably among the spectra; the ratios average near 60, with those obtained at the deep minima having lower values. The resolving power ($\lambda/\Delta\lambda$) is $\sim 45,000$ for the McDonald spectra, $\sim 35,000$ for the CTIO and KPNO spectra, and $\sim 45,000$ for the Keck spectra.

Each of the raw CCD images was trimmed, corrected for bias level, corrected for scattered light, divided by a normalized flat image from an incandescent lamp, wavelength cali-

TABLE 1
DETAILS OF SPECTROSCOPIC OBSERVATIONS

UT Date	HJD 2,448,000+	Pulse Phase ^a	Observation	CCD Detector/ Wavelength Range	HRV ^b (km s ⁻¹)	m_v ^c	Comments
1992 Jun 27	800.792	0.01, 0.59	CTIO	Tek 2048 3900-6000 Å	...	9.2	C ₂ bands in absorption
1992 Sep 11	876.776	0.67, 0.17	KPNO	Tek 2048 5350-8650 Å	43	10.7	No C ₂ bands
1993 Aug 8	1,207.764	0.55	McDonald	Reticon 400 × 1200 5800-7300 Å	44	11.4	
1993 Sep 3	1,233.714	0.77	McDonald	Reticon 400 × 1200 4370-4860 Å	...	11.2	C ₂ band in absorption
1993 Oct 9	1,269.668	0.09	McDonald	Reticon 400 × 1200 5760-7230 Å	44	11.4	
1993 Nov 1	1,292.630	0.29	McDonald	Reticon 400 × 1200 4140-4540 Å	...	11.3	
1994 May 1	1,473.933	0.87	McDonald	Reticon 400 × 1200 5030-5900 Å	...	12.9	Strong Na I emission, C ₂ bands in emission
1994 May 2	1,474.933	0.88	McDonald	Reticon 400 × 1200 6400-8600 Å	42	12.8	H α emission
1994 May 24	1,496.841	0.07	McDonald	Reticon 400 × 1200 5550-6900 Å	47	13.4	Strong Na I emission, C ₂ bands in emission
1994 Jul 29	1,562.739	0.65	McDonald	Reticon 400 × 1200 5700-7200 Å	46	12.3	Na I emission, no H α emission
1994 Aug 16	1,580.777	0.16	McDonald	Reticon 400 × 1200 5700-7200 Å	45	13.0	Na I emission, no H α emission
1994 Oct 21	1,646.588	0.38	McDonald	Reticon 400 × 1200 6200-8200 Å	40	12.8	
1995 Oct 12	2,002.600	0.49	CTIO	Loral 3K 5550-8200 Å	46	11.3	C ₂ bands in absorption
1995 Dec 10	2,061.561	0.01	McDonald	Reticon 400 × 1200 5000-5900 Å	...	10.6	C ₂ bands in absorption
1996 Jun 10	2,245.039	0.62	Keck	Tek 2048 4300-6620 Å	41	15.3	Strong Na I emission, C ₂ bands in emission
1996 Nov 13	2,400.568	0.98	McDonald	Reticon 400 × 1200 6200-8220 Å	40	12.1	
1996 Nov 14	2,401.559	0.99	McDonald	Reticon 400 × 1200 5460-6760 Å	41	12.1	C ₂ band in absorption
1996 Dec 5	2,422.544	0.18	McDonald	Reticon 400 × 1200 5720-7220 Å	41	12.1	

^a Phase zero corresponds to minimum light. The phases were calculated from the ephemerides of Arhipova 1996; her eq. (2) ($JD_{\min} = 2,449,030 + 114.875E - 0.04167E^2$) was applied to all the spectra, and eq. (1) was also applied to our two 1992 spectra.

^b HRV is the heliocentric radial velocity. It was measured in the 6410-6440 Å region by comparison to a synthetic spectrum. The typical uncertainty of a velocity estimate is ± 1 km s⁻¹.

^c The visual magnitude estimates are derived from the same data sets used to construct Fig. 1.

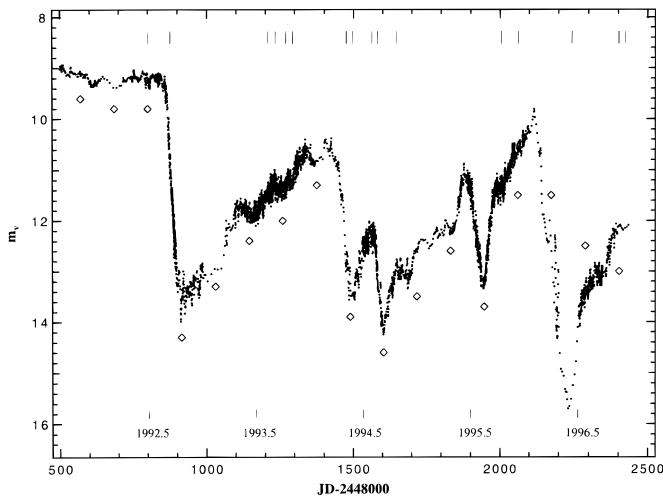


FIG. 1.—Visual photometry of FG Sge covering the time span of our spectroscopic observations. The data points are the result of a five-point running average applied to the combined (after placing the different data sets on the same zero-point scale) observations from the AAVSO (J. Mattei 1997, private communication), AFOEV, BAAVSS, and VSOLJ. The epochs of the spectroscopic observations are indicated by vertical lines along the top of the diagram. The light minima calculated with Arkhipova's (1996) ephemeris (her eq. [2]) are indicated with diamond symbols.

brated, continuum normalized, and transformed into one-dimensional spectra using the programs in the ECHELLE package of the standard astronomical data analysis facility, NOAO IRAF. The wavelength scale was calibrated with Th-Ar lamp spectra taken immediately following each observation of FG Sge. The precision of the wavelength calibration is typically about 0.005 \AA . Hot star spectra were also obtained (during most, but not all runs) and used to divide out the telluric lines from the spectra of FG Sge. Given the high density of lines in the spectra of FG Sge, the continuum is not very well defined in most regions. We normalized them by dividing by a low-order function, which was fitted through the high points that were not obviously due to cosmic rays or emission features. This procedure gave satisfactory results based on comparison of spectra obtained during different observing runs and also based on comparison of overlapping regions of adjacent orders.

3. ANALYSIS

3.1. Recent History of FG Sge and Qualitative Descriptions of the Spectra

3.1.1. Introduction

Wallerstein (1990) and Kipper & Kipper (1993) have shown that most of the absorption lines in the spectrum of FG Sge belong to the first ionization spectrum of the rare earths. In fact, the (usually) strong and unblended Fe I and Fe II lines, which are often used in abundance studies of normal F and G stars, are mostly severely blended with lines of Ce II, Pr II, Nd II, Sm II, etc. FG Sge experienced the first of a series of sudden brightness declines beginning on 1992 August 26 that have continued until the present. Our spectra of FG Sge obtained before the 1992, 1994, and 1996 fadings are generally characterized by a high density of absorption lines of moderate strength. The spectra obtained during the deep minima of 1994 and 1996 display emission lines superimposed on a weak continuum. In the following,

we briefly give an overview some of the spectroscopic variations exhibited by FG Sge since 1992 June, the date of our first observation. We begin with a discussion of its most recent pulsational behavior.

3.1.2. Pulsations

Since the first half of this century, FG Sge has exhibited low-amplitude brightness variations in addition to its gradual century-long brightening (van Genderen & Gautschy 1995). They have been attributed to quasi-periodic pulsation, because FG Sge also exhibits color and velocity variations that vary in phase with the brightness variations (Arkhipova 1996). The pulsation period (P) has steadily increased this century until recent times—see Kipper (1996, Fig. 1) showing P near 30 days in 1965 and increasing to about 100 days by the late 1980s. Van Genderen & Gautschy claim that it dropped to about 65 days starting in 1991. However, Arkhipova (1996), using Fourier analysis and being careful to correct for aliasing, finds that P has remained near 110 days through the 1990s. The sparse velocity measurements available (Cohen, Marcy, & Harlan 1980 and ours) indicate that the velocity has a peak-to-peak variation of $\sim 4\text{--}6 \text{ km s}^{-1}$.

We have combined the visual brightness estimates from four amateur variable star groups to create a single light curve for FG Sge covering the Julian date range 2,448,500–2,450,500: American Association of Variable Star Observers (AAVSO), Association Francaise des Observateurs d'Etoiles Variables (AFOEV), British Astronomical Association Variable Star Section (BAAVSS), and Variable Stars Observers League in Japan (VSOLJ). The lower limit magnitude estimates were removed from the data bases. The total numbers of observations from each group retained for analysis are 443 (AAVSO), 1554 (AFOEV), 294 (BAAVSS), and 2927 (VSOLJ). This results in an average of nearly three observations per night! The zero-point offsets among the data sets have been determined by comparing the average magnitudes in the Julian date range 2,449,100–2,449,300, where the four data sets have significant overlap; we have defined the VSOLJ data set as the “standard.” The offsets are less than 0.1 mag, on average. In addition to visual magnitude estimates, the data sets contain photoelectric and CCD measurements. The typical difference between a visual estimate and a photoelectric measurement obtained on the same night is ~ 0.2 mag, which we take as the average uncertainty of a single visual estimate. The CCD measurements are useful especially when FG Sge drops below ~ 14 mag (such as in 1996 June), when it becomes difficult to follow visually and photoelectric measurements might be contaminated by the extended nebular emission. We present the final light curve in Figure 1.

We confirm Arkhipova's discovery that the timing of the four major fadings between 1992 and 1995 are well described by her equation (2), which is an ephemeris with a nearly constant P of about 115 days (but note that deep fadings do not occur at every cycle). Several of the low-amplitude brightness variations occurring since the deep 1992 fading are also well described by the ephemeris (see Fig. 1). This possible link between the pulsation of FG Sge and its deep fadings is significant, because it implies a causal link between the two. The fadings start near maximum light and reach minimum light in about half a pulsation cycle. The ephemeris fails for the very deep minimum of 1996

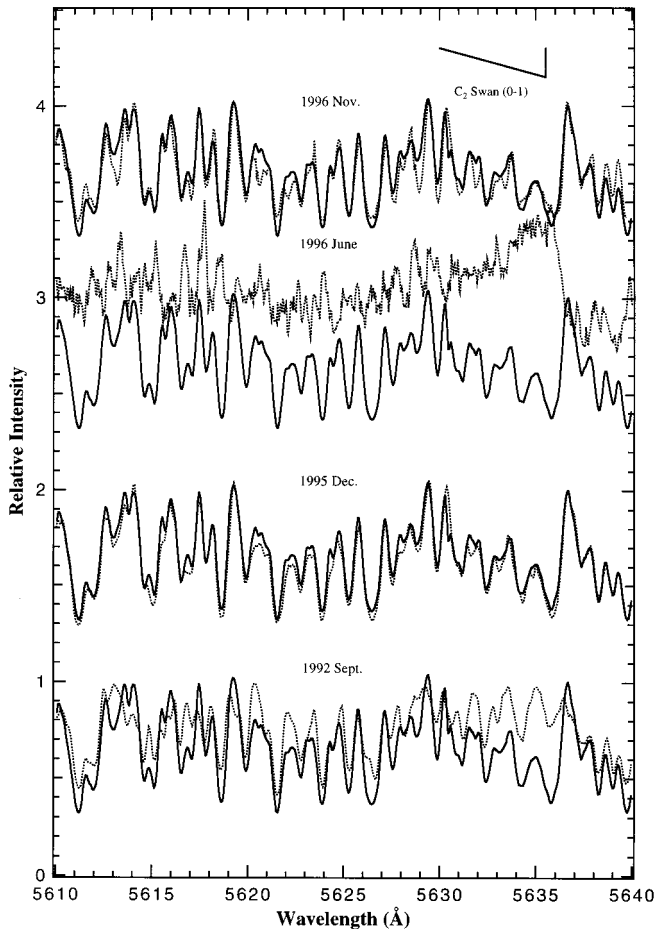


FIG. 2.—Variation of C_2 Swan 0–1 band head strength since 1992 June. The 1992 June (solid curve) is overplotted on all the other spectra (dotted curves). The C_2 band head was present in emission in the 1994 May and 1996 June spectra.

June, though, possibly indicating that a substantial change in P occurred at that time or simply that the deepest fadings are not always connected to the pulsation. The predicted minimum immediately preceding the 1996 fading apparently did coincide with a “hesitation” in the decline to minimum light. We list in Table 1 the pulsation phases of our spectra calculated from Arkhipova’s ephemerides (her eqs. [1] and [2]).

3.1.3. Molecular Bands

The C_2 molecular bands have varied greatly in strength in the spectra of FG Sge, sometimes disappearing completely, since their first detection in 1980 August (Acker, Jaschek, & Gleizes 1982). The C_2 Swan 0–1 band head at 5635 Å disappeared⁴ sometime before our 1992 September 11 spectrum (Fig. 2) but after 1992 August 9, when Iijima (1996) reported a detection of C_2 . On three occasions, 1995 October, 1995 December, and 1996 November, the C_2 bands in our spectra have returned to their predecline strength. Iijima and Iijima & Strafella (1993) review the changes in the C_2 band strengths in their moderate-resolution spectrophotometric observations from the early 1980s until 1994; Iijima reports that the C_2 bands were

⁴ The disappearance of the C_2 bands in 1992 September is probably not due to filling-in by C_2 emission, because “chromospheric” emission was not seen during the 1992 decline (see § 3.1.5).

strong on 1992 December 16, 1994 April 23, and 1994 December 25 and absent on 1993 August 15. Kipper, Kipper, & Klochkova (1995) report that the C_2 bands are strong in their 1994 August spectra. Combining all these reports, we note that the C_2 band heads are weakest during a narrow phase interval centered at about 0.65, and they gradually rise back to maximum strength by phase 1.0 (minimum light).

For the first time, we have detected the C_2 bands in emission in the spectrum of FG Sge (Fig. 2), which occurred during the deep brightness declines of 1994 May and 1996 June. Significantly, C_2 emission was not seen during the 1992 decline.

There is no evidence of the $^{12}C^{13}C$ band head at 5625.6 Å based on examination of the 1996 June spectrum (we get $^{12}C/^{13}C \geq 10$), which has prominent $^{12}C^{12}C$ band heads at 5165 Å and 5635 Å in emission. Iijima & Strafella had reported the presence of $^{12}C^{13}C$ and $^{13}C^{13}C$ absorption bands in their low-resolution spectra of FG Sge, but Iijima (1996) retracted that claim, noting that these previously identified band heads were due instead to strong rare earth lines.

The CH band head at 4310 Å appeared weakly in emission in our 1996 June spectrum. Iijima did not note the presence of CH in his spectra.

We did not see CN lines, but our blue coverage, where the CN lines would be strongest, is poor. Iijima claimed to see a weak CN band head at 4215 Å in 1994 April, when the C_2 absorption bands were strong.

3.1.4. Na I D Lines

Regarding the Na I D lines, more gradual but still dramatic changes have occurred since 1992 June (Fig. 3). Before the 1992 decline two components were seen, both in absorption: (1) sharp interstellar lines, and (2) slightly broader absorption lines coinciding with the photospheric velocity. In 1992 September, the photospheric lines had narrowed considerably. By 1993 August, very broad blueshifted absorption components of the Na I D lines began to appear; simultaneously, the narrow photospheric absorption components disappeared. Kipper et al. (1995) had also noted the appearance of broad blueshifted absorption components in their spectra of 1994 August. These broad components have remained detectable until our most recent spectrum (1996 December). In the 1993 August spectrum they were blueshifted by 140 km s⁻¹ relative to the original (1992 June) photospheric components, and they had a FWHM of about 55 km s⁻¹. By 1996 December the blueshifted component had widened to about 140 km s⁻¹ with a mean blueshift of about 205 km s⁻¹. This far exceeds the escape velocity at the surface of FG Sge (~65 km s⁻¹, calculated using HB’s luminosity and reddening, our temperature, and Blöcker & Schönberner’s 1997 mass estimates). Like the C_2 bands, the photospheric Na I D lines in 1995 December are nearly identical in appearance to the those in 1992 June (except for the broad blueshifted components). In the middle of the 1994 May and 1996 June declines, very strong Na I D emission—sharp and broad—lines dominated the local spectrum.

3.1.5. Spectra during the Deep Minima

Curiously, apart from the lack of C_2 lines, the spectrum we obtained during the 1992 decline is very similar to our predecline spectrum. Emission lines are prominent in the

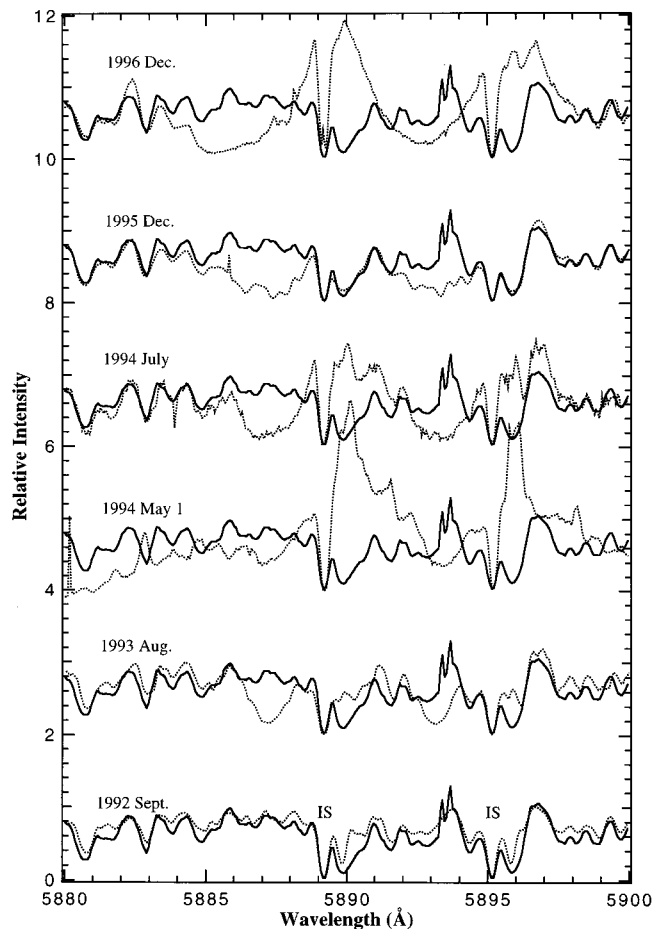


FIG. 3.—Evolution of the Na I D lines since 1992 June. The 1992 June spectrum (solid curve) is overplotted on all the other spectra (dotted curves). The spectra have been shifted in velocity so that the interstellar lines (indicated by IS) are at the rest wavelength. Note the appearance of a broad blueshifted absorption component and the disappearance of the sharp stellar component in the 1993 August spectrum. The sharp emission features at ~ 5893 Å in the 1992 June and at ~ 5889 Å in the 1996 December spectra are artifacts unrelated to the intrinsic stellar spectra.

1994 May and especially 1996 June (Fig. 4) spectra. The Na I D emission lines were by far the strongest emission lines. The emission lines of Sc II and Ti II in the 1996 June spectrum are comparable in strength to the emission lines of the rare earths. We did not detect any helium emission lines in the 1996 June spectrum (or in any other spectra). In the 4200–4500 Å region of the 1996 June spectrum only those Fe I lines with large gf -values and $\chi_{\text{upp}} \leq 4.5$ eV are present. If the atomic populations are due to LTE thermal collisions, then it appears that the excitation of the emission lines seen during the 1996 minimum is similar to that of the absorption lines seen outside the deep minima.

The heliocentric radial velocity of the rare earth emission lines in the 1994 May and 1996 June spectra is near the average value measured for the absorption spectra outside minimum light. This implies that the region producing the rare earth emission lines during the deep minima is not experiencing significant expansion and might be participating in the same pulsational motion as the photosphere. The chromospheric emission lines in the 1996 June spectrum are fully resolved, with a FWHM of about 15 km s^{-1} .

Unlike the chromospheric emission lines, the nebular (Balmer lines, [N II], [O III]) and Na I D emission lines in

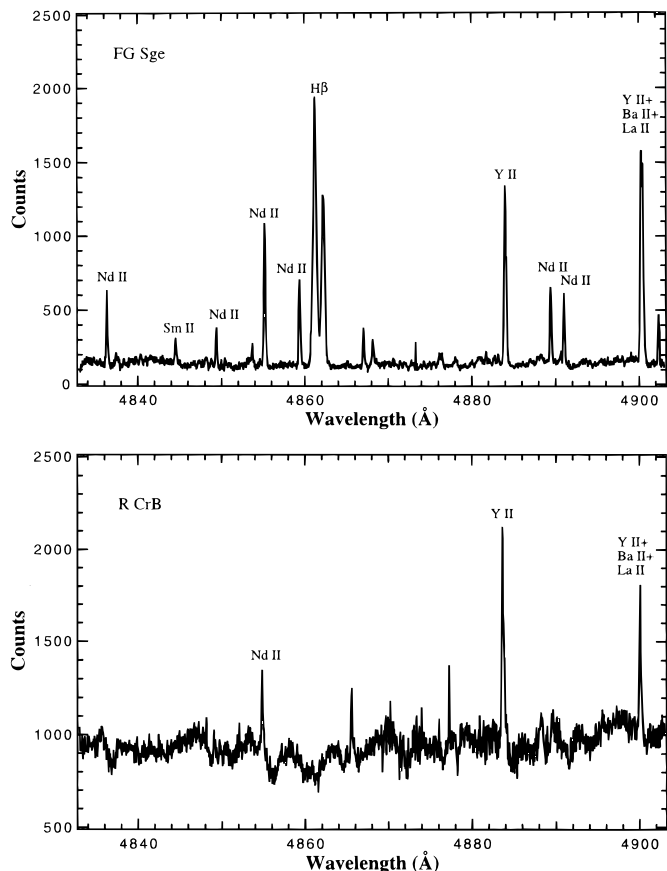


FIG. 4.—Portion of the 1996 June spectrum of FG Sge is shown in the first panel. The H β line is produced in the fossil nebula. A spectrum of R CrB from February 1996 (in the middle of a deep minimum) is shown in the second panel. Some absorption lines are weakly present in the spectrum of R CrB.

the 1996 June spectrum exhibit complex structure. The hydrogen Balmer and [N II] lines display two components, and the [O III] lines show at least five (Fig. 5). The two highest velocity components of [O III] are at about $\pm 40 \text{ km s}^{-1}$ relative to the rare earth lines. The expansion velocity, determined from the [N II] lines, is $35 \pm 1 \text{ km s}^{-1}$ (it is about 2 km s^{-1} less for the H α line), and their mean velocity is $41 \pm 1 \text{ km s}^{-1}$ —in good agreement with Flannery & Herbig's (1973) measured expansion velocity of 34 km s^{-1} and mean nebular velocity of 38 km s^{-1} using the same lines. This nebular velocity is very close to the mean photospheric velocity of FG Sge (see Table 1).

We discovered a new phenomenon in FG Sge in our 1994 May 1 spectrum: it is a near-perfect mirror image of the 1992 June spectrum. In Figure 6 we have overplotted the inverse of this spectrum on the 1992 June spectrum. The 1994 May 1 spectrum was obtained during the rapid decline to minimum. This is reminiscent of the solar eclipse chromospheric spectrum, where obscuration of the photospheric continuum light leads to an emission spectrum. Examination of the strong Ba II line at 5853 Å in the 1 May spectrum revealed that it was still weakly present in absorption, even though the other lines had already gone into emission. By May 24, the Ba II absorption line had disappeared.

An unexpected benefit of observing FG Sge during a deep minimum was our ability to image the faint nebula around FG Sge, which we present in Figure 7 (Plate 1).

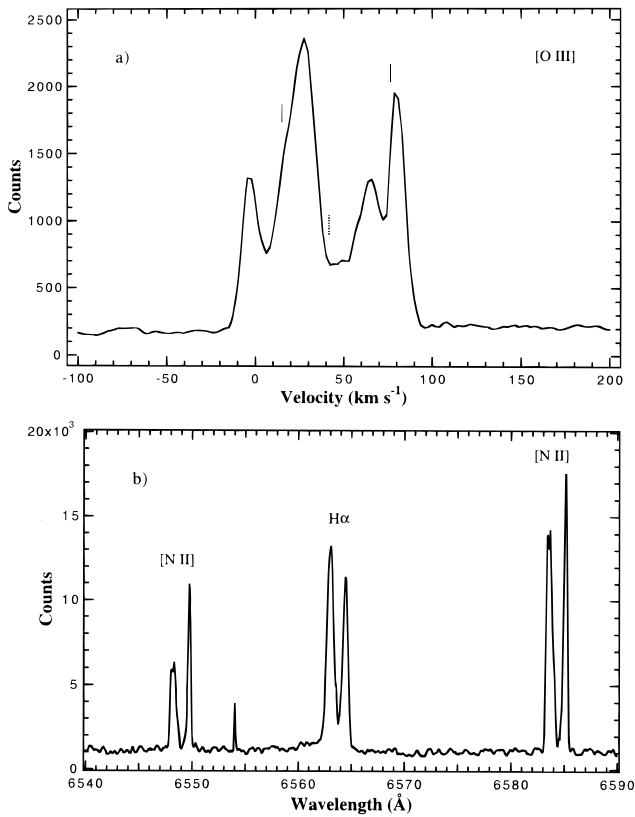


FIG. 5.—Velocity profile of [O III] emission line at 5006.84 Å (a). The velocity of the emission lines of the rare earths is indicated by a dotted line and the velocities of the H β components by solid lines. The velocities have been corrected for the Earth's motion. The H α region is shown in (b). Both regions are from the 1996 June spectrum obtained during the very deep minimum.

3.2. Abundance Analysis

3.2.1. Atmospheric Parameters and Atomic Abundances

The first step in any abundance analysis is the determination of the physical parameters of the star in question. This is usually approached in two ways: (1) the temperature

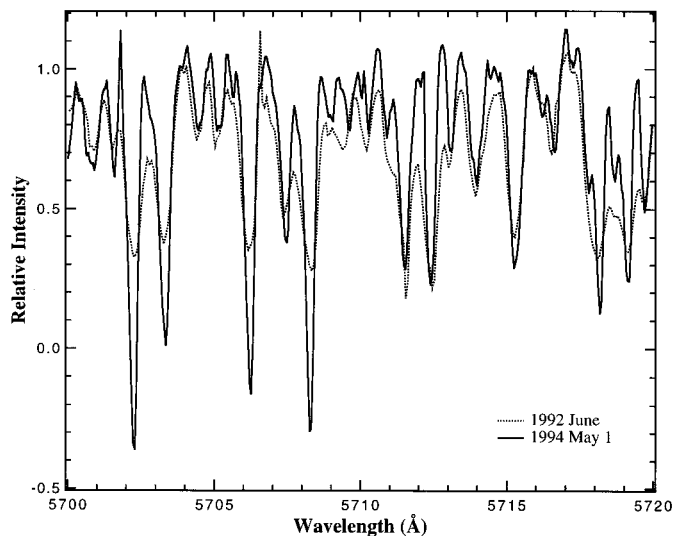


FIG. 6.—Emission-line spectrum from 1994 May 1 has been inverted and overplotted with the 1992 June spectrum. The spectral resolutions have been matched; hence, the apparent line-width differences are real.

and surface gravity can be derived from photometry (or spectrophotometry) and assumptions concerning the mass and luminosity, or (2) both temperature and surface gravity can be determined from a curve-of-growth type of analysis using equivalent widths, W_λ 's, of the Fe I and Fe II lines.

Previous studies of FG Sge have employed a number of methods for estimating its effective temperature (T_{eff}). HB applied standard spectral type classification techniques to estimate T_{eff} ; by 1965, FG Sge had reached a spectral type of A3 Ia and was cooling at a rate of about 250 K per year. Until the early 1970s, the absorption lines were much easier to measure than they are now. Langer et al. (1974) reported that estimates of T_{eff} derived from the continuous energy distribution, the width of the H α line, and the unreddened values of $B-V$ and $U-B$ all agreed with each other until early in 1970, when they began to diverge. Given the increased line-blanketing by rare earths after 1970, it is not surprising that the various temperature indicators began to give inconsistent results. Thus, estimates of T_{eff} obtained from FG Sge's colors by some investigators (van Genderen 1994; van Genderen & Gautschy 1995) are not likely to be reliable. The basic problem is the lack of a suitable comparison object with known physical parameters. The Balmer line profiles may also give unreliable temperatures if the atmosphere of FG Sge is H deficient (see § 4.2). In any case, the high density of absorption lines makes it difficult to trace the Balmer line wings accurately (see § 3.1.5).

Probably the most accurate published temperature estimates since the early 1970s are those of Montesinos et al. (1990). They analyzed ultraviolet *IUE* spectra obtained between 1982 and 1989 and showed that FG Sge maintained a roughly constant temperature and might even have warmed slightly. Montesinos et al. found satisfactory agreement between the *IUE* spectra and an older Kurucz model atmosphere (Kurucz 1979) with $T_{\text{eff}} = 6500$ K and $\log g = 1.5$; their infrared *JHKL* measurements yielded the same T_{eff} . Kipper & Kipper (1989) also concluded that the spectral type had not changed during the 1980s. Combined with the near constancy of the quasi-pulsation period during this time, implying constancy in the mean radius, these observations suggest that the present mean atmospheric parameters of FG Sge are close to what they were in the late 1980s. It should also be noted that in 1992 a strong infrared excess appeared (Woodward et al. 1993), which has rendered the infrared fluxes useless for estimating T_{eff} for FG Sge.

Since we cannot use the colors of FG Sge to estimate its atmospheric parameters, we first attempted the traditional Fe line analysis method. We searched for relatively clean Fe I and Fe II absorption lines in the 1994 October 21 spectrum, which appears to have a better defined continuum than the other spectra and has a relatively high S/N. However, we were not satisfied with the quality of the analysis due to the small number of unblended lines and the large line-to-line scatter in the derived abundances. Therefore, we have chosen another, hopefully more reliable, method for determining the atmospheric parameters, which we describe next.

Throughout the abundance analysis we employ an updated version of the LTE stellar abundance code, MOOG (Snedden 1973). It has two modes of operation, standard single-line analysis and spectrum synthesis. In the first mode, the W_λ values of isolated absorption lines are given as input, and in the second mode, a synthetic spectrum is gen-

erated and overplotted on the observed spectrum. We have selected the second mode of operation, given the amount of line crowding in our spectra of FG Sge. We use the Kurucz (1993) LTE plane-parallel stellar atmospheres with scaled solar abundances⁵ as input into MOOG. We derived the oscillator strengths, gf -values, of elements up to Ni in the same manner as Gonzalez & Lambert (1996), who used the solar spectrum to calculate gf -values with a Kurucz model of the solar atmosphere; the procedure involves matching the solar spectrum by adjusting the gf -values of an extensive line list, in our case, the Kurucz (1989) line list, which is an updated version of the Kurucz & Petrymann (1975) line list. Since the strongest lines in the spectrum of FG Sge belong to the heavy elements, which are very weak or absent in the solar spectrum, their gf -values were not altered from the original Kurucz (1989) tabulations, some of which are from laboratory values of Corliss & Bozman (1962)⁶; we list in Table 2 the gf -values of the heavy elements used in the analysis, along with the adopted solar abundances for each element. When improved gf -values of these lines become available, it will be easy to update our abundance estimates.

Because of severe line crowding, we must use spectrum synthesis to disentangle the Fe I and Fe II lines from the more numerous lines of the rare earths. Using the tabulations of Moore, Minnaert, & Houtgast (1966) and Wallerstein (1990) as a guide, we selected in our 1994 October 21 spectrum what appears to be the best region for estimating T_{eff} and surface gravity, g : 6405–6440 Å. This region contains two relatively clean Fe I lines, at 6419.95 Å and 6421.35 Å, with significantly different lower excitation potentials. It also contains three blended Fe I lines and two blended Fe II lines. The relative strengths of the Fe I lines are sensitive primarily to T_{eff} and to the microturbulence velocity parameter, ξ_t . Given T_{eff} , the relative strengths of the Fe I and Fe II lines are primarily sensitive to g . After several iterations, we settled on a solution which resulted in the minimum residual between the observed and synthetic spectra: $T_{\text{eff}} = 6500$ K, $\log g = 2.0$, $\xi_t = 5.0$ km s⁻¹, and $[\text{Fe}/\text{H}] = -0.1$. Our T_{eff} estimate is close to the quantitative estimate of Montesinos et al. (1990) and the qualitative estimate of Kipper & Kipper (1989). Our adoption of $\xi_t = 5.0$ km s⁻¹ is based in part on the fact that most supergiants have ξ_t values in the range 3–4 km s⁻¹: Gonzalez & Lambert (1996) estimated $\xi_t = 3.4$ km s⁻¹ for α Per. This is in contrast to Kipper & Kipper's estimate of 11 km s⁻¹ based on the Nd II lines. We present in Figure 8 our synthesis of the 6405–6440 Å spectral region overplotted with the 1994 October 21 spectrum.

We estimate the uncertainties in the parameters, T_{eff} , $\log g$, and ξ_t , to be 400 K, 0.5, and 2.0 km s⁻¹, respectively. These uncertainties are based primarily on the behavior of the Fe I and Fe II line strengths as the atmospheric parameters are changed. The uncertainty in $[\text{Fe}/\text{H}]$, based on the uncertainties in the atmospheric parameters and on the continuum placement, is about 0.3 dex. The uncertainties in

TABLE 2
ATOMIC DATA FOR LINES OF HEAVY
ELEMENTS USED IN THE
ABUNDANCE ANALYSIS

Species, log ϵ_{\odot} Wavelength (Å)	χ_i (eV)	log gf
Ga I, 3.15:		
6413.47	3.07	-0.30
Sr I, 2.95:		
6408.46	2.27	0.71
Y I, 2.25:		
6435.00	0.07	-0.82
6664.40	3.09	0.39
6687.57	0.00	-2.00
6694.83	2.29	-1.43
Zr II, 2.63:		
6346.48	2.41	-1.30
6677.92	2.42	-1.36
Nb I, 1.42:		
6430.44	0.74	-1.23
6660.83	1.18	-0.97
Mo I, 1.98:		
6424.35	2.50	-1.00
7244.58	3.25	-1.96
7245.85	2.50	-1.22
La II, 1.22:		
6358.11	0.71	-1.94
6636.52	0.93	-2.27
6642.76	2.53	-0.96
6671.40	0.40	-2.03
Ce II, 1.63:		
6343.96	0.33	-2.17
6425.28	2.23	-0.80
6652.74	1.53	-1.21
6744.71	1.68	-1.24
6754.97	1.68	-1.81
7238.37	1.54	-1.24
Pr II, 0.80:		
6244.36	1.20	-0.72
6347.11	1.59	-0.55
6255.10	1.26	-0.77
6413.68	1.13	-0.85
6429.63	1.62	-0.33
6431.81	1.42	-0.52
6584.56	1.59	-1.24
6656.83	1.82	0.08
6673.41	1.62	-0.26
6673.73	1.42	-0.32
7227.69	1.62	-0.66
Nd II, 1.49:		
6248.27	1.22	-1.60
6250.44	1.16	-1.62
6258.72	1.32	-0.98
6341.49	1.80	-0.52
6425.78	1.65	-0.61
6428.65	0.20	-1.65
6580.93	1.44	-1.09
6585.70	1.44	-1.08
6588.02	1.77	-0.80
6591.43	0.20	-2.51
6636.18	2.06	-0.76
6637.19	1.45	-1.08
6650.52	1.95	-0.17
6669.63	1.04	-1.72
6678.52	1.52	-1.21
6680.14	1.69	-0.81
6698.64	1.64	-1.36
7236.55	0.06	-2.66
Sm II, 0.99:		
6244.13	1.08	-2.10
6246.75	1.06	-1.86
6256.59	1.17	-1.75
6353.48	1.30	-1.94
6357.23	1.35	-1.78
6406.25	1.36	-1.70
6417.48	1.08	-2.05

⁵ This means that we assume a normal H abundance for the atmosphere of FG Sge. Hence, the number density abundances quoted as log ϵ are scaled such that log $\epsilon(\text{H}) = 12.0$ and log $\epsilon(\text{He}) = 11.0$. If the atmosphere of FG Sge turns out to be H deficient, then one can scale the abundances to log $\Sigma \epsilon_i \mu_i = 12.15$. We are planning a future study of FG Sge making use of H-deficient model atmospheres.

⁶ It has long been known that uncertainties near a factor of 2 exist in the Corliss & Bozman (1962) tabulations (Corliss & Bozman, pp. XIV and XV and Takens 1970).

TABLE 2—Continued

Species, log ϵ_{\odot} Wavelength (Å)	χ_1 (eV)	log gf
6428.36	1.37	-0.88
6431.01	1.36	-1.89
6431.98	1.41	-2.18
6585.20	1.17	-1.84
6589.71	1.27	-1.30
6630.62	1.52	-1.95
6632.28	1.67	-1.34
6649.04	1.38	-1.93
6651.63	1.46	-1.85
6656.16	1.17	-2.01
6667.22	1.26	-2.12
6679.22	1.08	-1.69
6681.53	1.41	-1.97
6687.80	1.71	-1.68
6693.56	1.69	-1.09
6694.72	1.37	-2.21
6741.50	1.00	-1.88
6754.67	1.46	-1.93
7237.03	1.52	-2.02
7240.89	1.46	-1.41
Eu II, 0.57:		
6437.63	1.32	-0.20
6437.70	1.32	-0.01
6645.06	1.38	0.20
Gd II, 1.09:		
6346.64	1.31	-1.67
6422.40	2.62	-0.47
6634.33	1.31	-1.43
6679.53	2.55	-0.91
6681.20	1.43	-1.48
6694.89	2.60	-1.08
6752.65	2.33	-0.44
6753.89	2.49	-0.83
7242.22	1.17	-2.53
Tb II, 0.35:		
6645.37	1.69	-0.80
Dy II, 1.17:		
6594.15	1.85	-1.57
6654.23	2.18	-1.55
7234.68	2.57	-1.45
Er II, 0.97:		
6690.00	2.57	-1.05
Yb II, 0.97:		
6246.96	4.15	-0.42
6432.73	4.01	-0.75
Lu II, 0.14:		
6242.31	3.83	0.04
Hf II, 0.75:		
6248.92	1.50	-1.62
6644.58	1.78	-1.55
6647.06	2.87	-1.12
Pb I, 2.07:		
7228.97	2.66	-0.82

the log gf -values are difficult to gauge but might reach 0.5 dex for some of the more exotic species, especially considering that some values are from Corliss & Bozman.

We also used the spectrum synthesis technique for the general abundance analysis. Because of the amount of time involved in synthesizing even a small region of the spectrum, we restricted the analysis to seven regions (listed in Table 3) of the 1994 October 21 spectrum. The regions were selected primarily on the basis of specific lines representing certain elements: the 6240–6260 Å region for one Sc II line and one Fe II line; the 6340–6360 Å region for one Zr II line; the 6405–6440 Å region for one Ca I line, one Ga I line, several Fe I and Fe II lines, one Sr I line, and one Eu II line; the 6580–6600 Å region for three C I lines; the 6630–6700 Å region for two Al I and one Eu II lines; the 6740–6760 Å

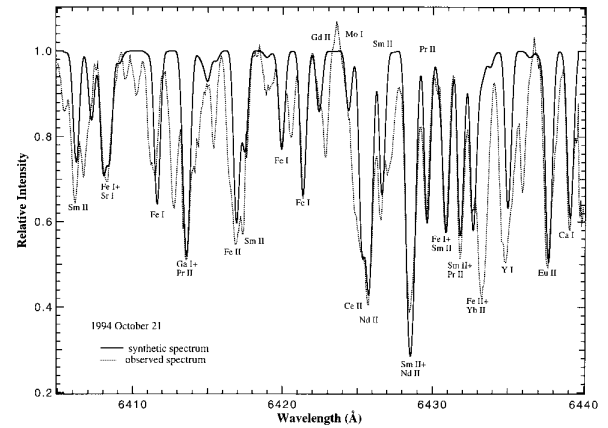


FIG. 8.—Sample region of the 1994 October 21 spectrum of FG Sge (dotted curve) overplotted with a synthesized version (solid curve), using the following atmospheric parameters: $T_{\text{eff}} = 6500$ K, $\log g = 2.0$, and $\xi_t = 5.0$ km s $^{-1}$. The labels identify the strongest features in the synthesized spectrum.

region for three S I lines; and the 7225–7250 Å region for one Pb I and two Mo I lines. Another criterion in our selection process is the presence of at least one discernible Fe line in each spectral region; however, this criterion was not fulfilled in every case (6340–6360 Å and 7225–7250 Å). Numerous lines of the heavy rare earth elements are well represented throughout all the spectral regions, so they were not an important consideration in selecting the regions. The line broadening (and, as discussed above, the atmospheric parameters) were established using the 6405–6440 Å region. We analyzed each spectral region independently of the others, adjusting the continuum level, radial velocity, and abundances to minimize the residuals between the observed and synthetic spectra. Since errors in the continuum placement among the different spectral regions would lead to systematic errors in [Me/Fe], we also adjusted the Fe abundance in each spectral region to match the few Fe I and Fe II lines present in them; thus, most systematic errors should cancel when the abundances of the elements are compared to Fe. We list the averaged results of the spectrum synthesis analysis in the last column of Table 3.

The abundance of lead is particularly important in stars enriched in the heavy s -process elements, because n -captures beyond lead cannot proceed on a slow timescale but, rather, result in a pile-up of ^{208}Pb (Clayton & Rassbach 1967). In order to test our identification of the absorption feature at 7229 Å as Pb I, we compare the 1994 October 21 and 1996 November 13 spectra (Fig. 9). The presence of strong C₂ bands in the 1996 November 14 spectrum suggests that FG Sge was near its minimum temperature at that epoch. All the lines appear stronger in the 1996 November spectrum, and it is more crowded; more significantly, though, the lines we have identified with neutral species are much stronger. Based on the appearance of the absorption feature at 7229 Å, we claim that it is probably a blend of two neutral lines separated by a few tenths of an Å, one of which is Pb I. As a final test, we generated syntheses of this spectral region using the abundances derived from the 1994 October spectrum and using a model with $T_{\text{eff}} = 5400$ K and $\log g = 1.7$, which produced the best solution; it yielded a relative increase in the strength of the neutral

TABLE 3
[Me/Fe] VALUES FOR THE 1994 OCTOBER 21 SPECTRUM OF FG SGE

SPECIES	SPECTRAL REGION							MEAN
	6240–6260 Å	6340–6360 Å	6405–6440 Å	6580–6600 Å	6630–6700 Å	6740–6760 Å	7225–7250 Å	
C I.....	0.98(3)	0.98
Al I.....	<0.8	<0.8
Si I.....	0.55(1)	0.35(2)	0.42
S I.....	0.14(3)	0.16(1)	0.14
Ca I.....	-1.04(1)	-1.04
Sc II.....	1.72(1)	1.72
Ni I.....	0.16(1)	0.16
Ga I.....	3.08(1)	3.08
Sr I.....	2.18(1)	2.18
Y I.....	3.28(1)	3.58
Zr II.....	...	3.50(1)	3.68(3)	3.20
Nb I.....	<4.0	...	2.90(1)	3.20
Mo I.....	4.05(1)	...	<3.7	<3.7
La II.....	4.05(2)	4.05
Ce II.....	...	3.11(1)	3.11(3)	3.11
Pr II.....	...	3.80(1)	3.40(1)	...	3.50(1)	2.90(2)	3.10(1)	3.27
Pr II.....	3.43(2)	...	2.73(2)	2.83(1)	2.93(3)	...	2.73(1)	2.96
Nd II.....	3.64(3)	3.44(1)	3.14(2)	3.34(4)	3.21(7)	...	3.64(1)	3.34
Sm II.....	3.34(3)	3.34(2)	2.94(4)	3.74(2)	3.46(10)	3.44(1)	3.14(1)	3.35
Eu II.....	1.66(1)	...	2.46(1)	2.06
Gd II.....	2.44(1)	...	3.09(4)	2.96
Tb II.....	2.98(1)	2.98
Dy II.....	3.16(1)	2.96(1)	...	3.26(1)	3.13
Er II.....	3.16(1)	3.16
Yb II.....	2.36(1)	...	2.58(1)	2.47
Lu II.....	3.59(1)	3.59
Hf II.....	3.28(1)	3.38(2)	2.58(1)	...	3.16
Pb I.....	3.53(1)	3.53

NOTE.—The [Me/Fe] values are listed for each spectral region followed by the number of lines of a given atomic species in that spectral region. The relative abundances listed in the last column are mean values weighted by the number of lines of a given species present in each spectral region.

lines approximately in agreement with the observed spectrum.

A search for the resonance lines of Tc I near 4300 Å in the 1992 June spectrum was not successful, owing to the very high density of strong rare earth lines in this region. We did set a limit of $\log \epsilon(\text{Tc}) < 1$ using a model atmosphere with

$T_{\text{eff}} = 5750$ K, $\log g = 1.5$, and $\xi_t = 4.0$ km s⁻¹, which yielded abundances of the elements similar to those derived from the 1994 October spectrum.

3.2.2. Synthesis of C₂ and CH Molecular Bands

As we showed in § 3.1.3, the C₂ molecular bands in the spectra of FG Sge have varied in strength considerably since they were first detected in 1980. The simplest explanation for this phenomenon is that they are due to variations in T_{eff} . In order to investigate this hypothesis, we have produced a difference spectrum of the 5630–5640 Å region, which is the difference between the 1992 June and September spectra (Fig. 10). Assuming that the C₂ lines do not contribute significantly to the September spectrum, then the difference should contain primarily C₂ lines with some residuals from neutral atomic lines, which are also temperature sensitive. We have generated synthetic spectra of the region containing the C₂ Swan 0–1 band head and compared them to this difference spectrum (Fig. 10). Using a model with $T_{\text{eff}} = 5500$ K, $\log g = 1.5$, $\xi_t = 5.0$ km s⁻¹, and $[\text{Fe}/\text{H}] = -0.1$, we find that $\log \epsilon(\text{C}) = 9.2$. Changing the temperature by ± 500 K leads to a change in the derived C abundance of ± 0.3 dex.

Assuming the disappearance of the C₂ bands during the 1992 decline was due primarily to a change in T_{eff} , then our syntheses imply that T_{eff} increased from ~ 5500 K in late 1992 June to at least 6000 K by 1992 mid-September. A temperature variation of about ± 500 K centered near 6000 K can easily account for the variation in C₂ strength seen in our other spectra and probably also in spectra going back to 1980. Certainly, these estimates are consistent with our analyses of the 7225 Å spectral region in the previous section. Combining these results with the trends we noted in

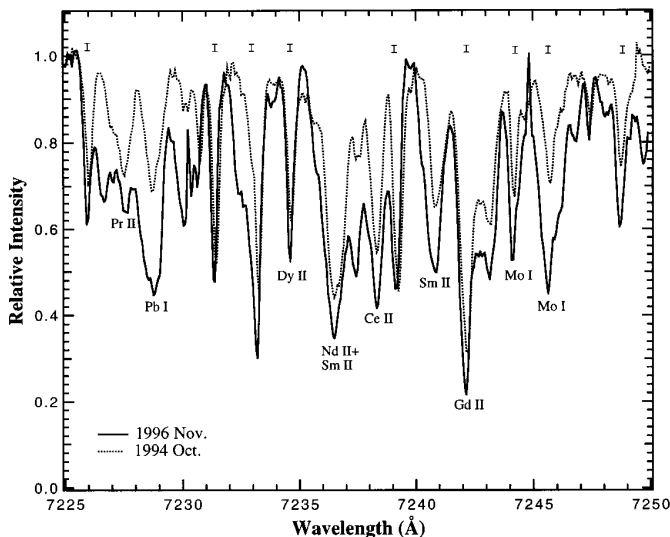


FIG. 9.—Comparison between 1996 November and 1994 October spectra containing the Pb I line at 7229 Å. The spectra have not been corrected for telluric absorption lines, which are indicated with I. The 1996 November spectrum contains strong C₂ bands (see Fig. 3), indicating the star was cool at this time. Note the relative strengths of the neutral and ionized lines.

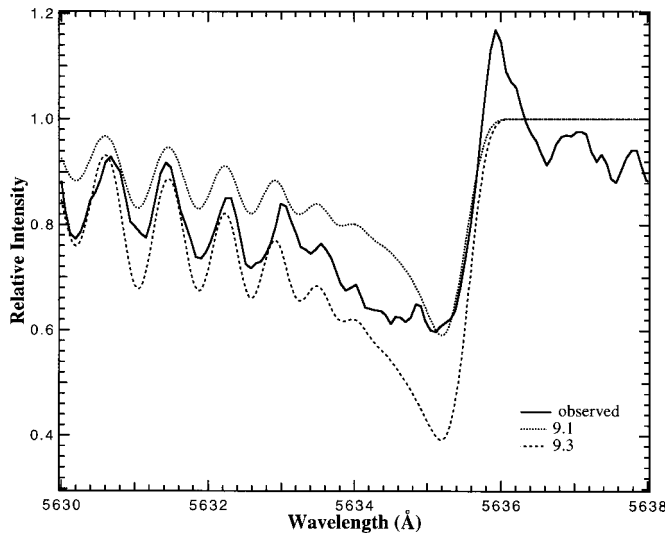


FIG. 10.—Difference between the 1992 June (strong C_2 absorption) and September (no C_2) spectra is indicated by a solid curve. Most of the residual absorption in this difference spectrum is due to C_2 . Synthetic line profiles calculated using $T_{\text{eff}} = 5500$, $\log g = 1.5$, $\xi_1 = 5.0 \text{ km s}^{-1}$, and $[\text{Fe}/\text{H}] = -0.1$ with two values of $\log \epsilon(\text{C})$, 9.1 and 9.3, are shown with dotted and dashed curves, respectively.

Section § 3.1.3 implies that the temperature reaches a sufficiently high value for the C_2 bands to disappear ($\sim 6500 \text{ K}$) only during a small fraction of the pulsation cycle of FG Sge. If the true value of $\log \epsilon(\text{C})$ were 9.5, easily within the range of uncertainty of our analysis, then the C_2 bands would still be strong even at 6000 K, which implies that the mean temperature would be greater than 6000 K.

We have also generated syntheses of the 4235–4335 Å region of the 1992 June spectrum in order to estimate the C abundance from the CH bands. Using the same model atmosphere quoted earlier for our determination of the Tc abundance, we derive $\log \epsilon(\text{C}) < 8.6$. A synthesis using $\log \epsilon(\text{C}) = 9.3$ yielded CH line strengths that are much too strong compared to the observed spectrum. Use of a lower temperature model atmosphere would have led to an even lower upper limit. The likely cause of this discrepancy, we will argue in § 4.2, is hydrogen deficiency in the atmosphere of FG Sge.

4. DISCUSSION

4.1. Abundances

4.1.1. Evolution of FG Sge's Abundances: 1970 to 1994

The abundances of the rare earth elements in FG Sge's atmosphere were greatly enhanced in the early 1970s, while abundances of the iron peak elements remained roughly constant at $[\text{Me}/\text{H}] \sim -0.2$ (Langer et al. 1974). In 1979 the absorption lines of the iron-peak elements appeared to weaken, while the lines of the rare earth elements remained strong (Cowley, Jaschek, & Acker 1985; Acker et al. 1982). About this time, Acker et al. first detected the C_2 bands.

The most thorough abundance analysis of FG Sge since Langer et al. is that of Kipper & Kipper (1993). Their estimates for the rare earth element abundances are, on average, about 0.5 dex greater than those of Langer et al. (from the 1972 spectrum), and their estimate for $[\text{Fe}/\text{H}]$ is about 0.3 dex less (but not significantly so, considering the uncertainties). Our abundance estimates are quite different

from those of Kipper & Kipper. While our estimate of $[\text{Fe}/\text{H}]$ is similar, we obtain a smaller value of $[\text{Ca}/\text{Fe}]$ and a larger value of $[\text{Sc}/\text{Fe}]$. Based on their syntheses of the C_2 bands, Kipper & Kipper estimated $\log \epsilon(\text{C}) = 9.3$, the same as our estimate, which is based on C I lines. However, our rare earth element abundances (expressed as $[\text{Me}/\text{H}]$) are, on average, about 1.2 dex greater! Given the uncertainties in the determination of the atmospheric parameters in both studies, it is not clear if these differences in the abundance estimates are significant. Not surprisingly, the $[\text{Me}/\text{Fe}]$ values are in better agreement. The differences between our abundance estimates and those of Langer et al. are almost certainly real, though. In particular, our carbon and rare earth abundance estimates are about 0.7 and 2.0 dex greater, respectively.

Especially surprising is our very high estimate for $[\text{Sc}/\text{Fe}]$ ($= 1.7$). Although our estimate is based on only one Sc II absorption line, the presence of Sc II lines in emission comparable in strength to the rare earth lines in the 1996 June spectrum is consistent with a high scandium abundance. Kipper & Kipper (1993) derived $[\text{Sc}/\text{Fe}] = 0.5$. Also, Cowley et al. went out of their way to note that Sc II was identified in their spectra with an unusually high confidence level and attributed this to an elevated scandium abundance.

4.1.2. The *s*-Process

Elements heavier than the iron group are overabundant by a large factor: $[\text{Me}/\text{Fe}] \sim 3$ from Table 3. This implies that the present atmosphere is composed of a substantial quantity of *s*-processed material (the level of *s*-process enrichment is 1–2 orders of magnitude higher than reported for AGB and barium stars). We assume that the composition of the atmosphere is effectively that of the processed material and unaffected by, for example, fractionation driven by separation of dust and gas (see below). The enhancement of the rare earths in FG Sge's atmosphere may be used to determine the neutron exposure, $\tau = \int n_n v_T dt$, that the iron peak elements have received in the *s*-processing region of FG Sge's interior. To accomplish this we present in Figure 11 the observed relative abundances [as $\log([\text{Me}/\text{Sm}])$] of the rare earths and several theoretical predicted distributions from Malaney (1987a, 1987b). The use of relative abundances reduces possible systematic errors in the analysis, since almost all of the rare earths lines are from singly charged ions of similar excitation. The exceptions are the neutral lines (e.g., Ga I, Sr I, Y I, and Pb I).

Malaney's calculations refer to different forms of exposure to neutrons. In one set, material of solar system composition is considered to be exposed once to neutrons with exposure given by the parameter τ : Figure 11 shows predicted $\log([\text{Me}/\text{Sm}])$ values for $\tau = 0.1$ and 1.0 mb^{-1} . In the second set, predictions are given for material exposed to an exponential distribution of neutron exposures characterized by the mean exposure τ_0 : Figure 11 shows predictions for $\tau_0 = 0.2$ and 0.4 mb^{-1} . A single exposure may be characteristic of *s*-processing that accompanies a final He-shell flash. An exponential distribution has been considered to be appropriate for thermally pulsing AGB stars (Ulrich 1973), but recent work suggests that this is not entirely true (Gallino et al. 1997).

The ratio of light *s*-process (Sr, Y, Zr) to heavy *s*-process (Ba and beyond) element abundances is a measure of the neutron exposure. The observed distribution is quite well

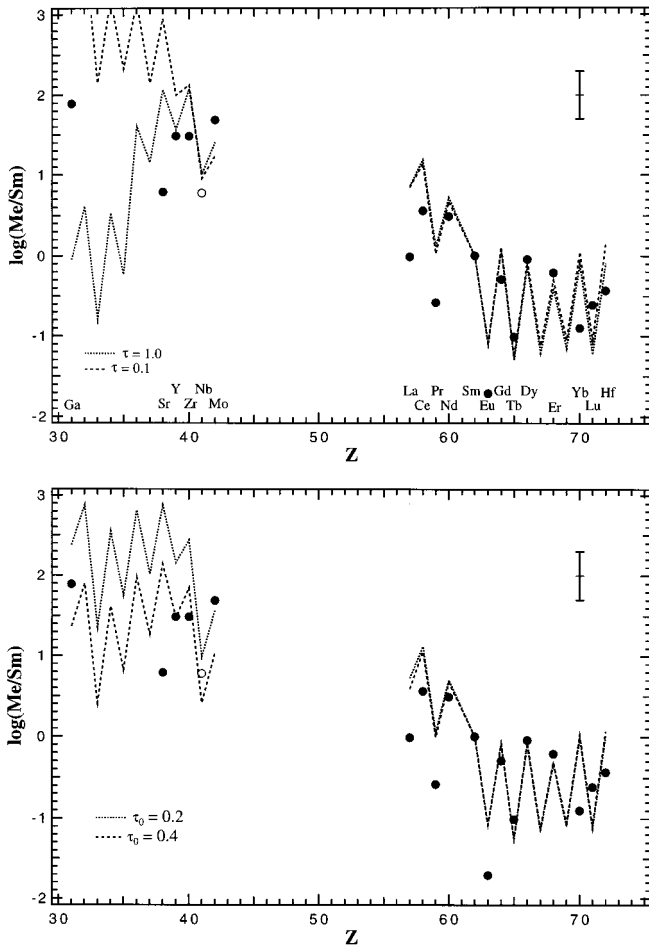


FIG. 11.—Logarithmic number density abundances of s -process elements relative to Sm in FG Sge (filled circles); the open circle represents an upper limit for the Nb abundance. An error bar with ± 0.3 dex is shown in the upper right of each diagram. Theoretical calculations from Malaney (1987a, 1987b) are also plotted.

described by a single neutron exposure of $\tau \sim 0.3 \text{ mb}^{-1}$, or a mean neutron exposure of $\tau_0 \sim 0.4 \text{ mb}^{-1}$. There are significant discrepancies, most notably Sr, La, Eu, and Yb. It is not surprising that the Sr and Yb abundances do not fit the models, given that they are based on one Sr I line and two low-quality Yb II lines. These neutron exposures apply to the s -processed material, as dilution by unprocessed material must be a minor effect.

We present Kipper & Kipper's (1993) results in Figure 12. The fit between the measurements and the models is quite good for $Z = 57\text{--}62$, but it is very poor for heavier rare earths. This discrepancy might be due either to misidentification and/or to improper treatment of line blending.

Malaney did not include technetium in his tabulations, so we cannot accurately compare our upper limit to the theoretical trend. Vanture et al. (1991), in their study of technetium in M and MS stars, find that $\log \epsilon(\text{Tc}) \sim 1.2$ in the stars with technetium. Unfortunately, our upper limit is near 1.0, so we cannot set useful constraints with this estimate.

One of the most important elements produced in the s -process is lead, because it marks the end of s -processing beyond which further n -captures lead to α -decays back to ^{208}Pb . Unfortunately, Malaney did not include the lead isotopes in his tabulations.

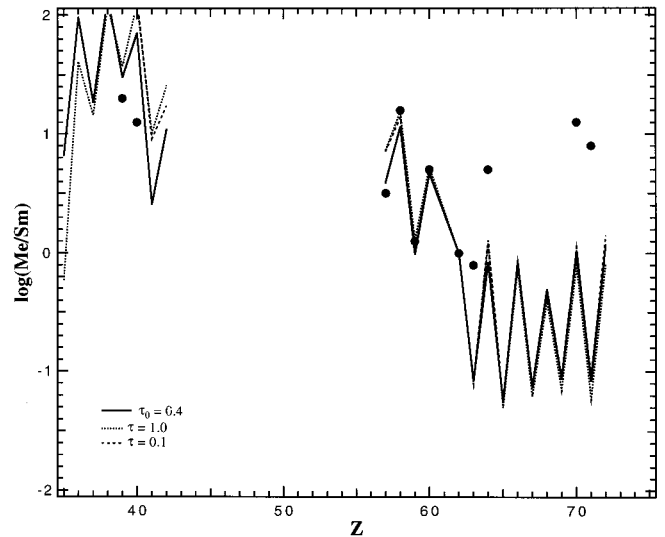


FIG. 12.—Same as Fig. 11, but using abundance estimates of Kipper & Kipper (1993).

The lack of any sign of ^{13}C in our spectra of FG Sge is potentially an important clue as to its nucleosynthesis and mixing history. The production of ^{13}C from ^{12}C in the H-burning shell and its subsequent destruction via $^{13}\text{C}(\alpha, n)^{16}\text{O}$ in the He-burning shell depend sensitively on the precise amount of mixing between the two shells (Renzini 1990 gives a brief overview of the process as it relates to R CrB stars). The presence of large s -process enhancements in FG Sge is certainly consistent with the absence of ^{13}C , since free neutrons are liberated when ^{13}C is destroyed.

4.1.3. Origin of Anomalous Scandium Abundances in FG Sge and Related Stars

As we noted above, the scandium abundance appears to be anomalously high⁷ in the atmosphere of FG Sge as determined directly from the absorption line spectrum by us and by Kipper & Kipper (1993) and as implied by the emission-line spectrum seen during the deep minimum of 1996 June. Asplund et al. (1997a) have reported an excess of scandium (as well as the light s -process products Sr–Zr) in Sakurai's object, a rapidly evolving luminous star, and Reddy et al. (1997) have reported large rare earth and moderate scandium overabundances in IRAS 05341+0852, a post-AGB candidate.

Scandium is normally one of the least abundant of the light elements; its abundance in typical stellar atmospheres is comparable to those of the rare earths. If a small quantity of a more abundant light element can be transmuted into scandium, then the scandium abundance can be significantly boosted. Specifically, a neutron capture by ^{44}Ca will produce ^{45}Sc , but further neutron captures on ^{45}Sc will deplete it. Owing to the much greater abundances of the calcium isotopes relative to scandium, the neutron captures

⁷ Here we use the phrase "anomalously high" in the sense that the scandium abundance in FG Sge is significantly greater than that seen in the general disk stellar population. Wheeler, Sneden, & Truran (1989), in reviewing published studies, quote a mean value of $[\text{Sc}/\text{Fe}] \sim 0$.

TABLE 4
NEUTRON CAPTURE CROSS SECTIONS
OF THE ISOTOPES USED TO
GENERATE FIGURE 13

Process Isotope	σ_n (mbarn)	Source
(n, γ) :		
^{40}Ar	2.43	1
^{39}K	20.15	1
^{40}K	45	2
^{41}K	49.29	1
^{40}Ca	12.06	1
^{41}Ca	40	2
^{42}Ca	25.87	1
^{43}Ca	129.2	1
^{44}Ca	12.53	1
^{45}Sc	195.3	1
(n, p) :		
^{40}K	35	2
^{41}Ca	12	2
(n, α) :		
^{40}K	180	2
^{41}Ca	1000	3

SOURCES OF NEUTRON CAPTURE CROSS SECTION DATA.—(1) Beer et al. 1992; (2) Woosley et al. 1978; see text for details; (3) Wagemans et al. 1995.

on calcium might outweigh the destruction of ^{45}Sc . We note the neutron-capture equilibrium value of $N(^{45}\text{Sc})/N(^{44}\text{Ca}) = \sigma(^{44}\text{Ca})/\sigma(^{45}\text{Sc}) = 0.064$, which is 2.4 times the solar ratio. In order to test this possibility, we have performed simple s -process calculations on a network of isotopes starting with ^{39}K using the standard set of coupled first-order differential equations (eq. [7-36] of Clayton 1983).⁸ We have adopted the neutron capture cross sections corresponding to a thermal energy of 10 keV, which is characteristic of the ^{13}C neutron source in low-mass AGB stars (Gallino et al. 1997). In addition to the (n, γ) reactions, we have also included the (n, p) and (n, α) reactions for the ^{40}K and ^{41}Ca isotopes, which have significant cross sections. The (n, γ) cross sections are from Beer, Voss, & Winters (1992), when available; otherwise, they are from Woosley et al. (1978). We note that Woosley et al.'s estimates for the odd isotopes are systematically larger than those of Beer et al.; we have adjusted the cross sections of the odd isotopes given by Woosley et al. to be in agreement with the scale of Beer et al.'s data (Table 4). The (n, p) and (n, α) cross sections are from Woosley et al. and Wagemans, Druyts, & Barthélemy (1995). The initial abundance for each isotope was set equal to the values given by Anders & Grevesse (1989), except iron for which we adopted $\log \epsilon = 7.50$ (the iron isotopes were handled with a separate network); the initial abundances of ^{40}Ar , ^{40}K , and ^{41}Ca were set to zero. We present the resulting variations of the isotopic and elemental abundances of Ar, K, Ca, Sc, and Fe with τ in Figure 13. We did not include Ca isotopes beyond ^{44}Ca , because ^{45}Ca decays into ^{45}Sc with a half-life of only 168 days. The critical neutron density above which ^{45}Ca is transmuted into ^{46}Ca is $\sim 3 \times 10^9 \text{ cm}^{-3}$. Gallino et al. estimate that the

⁸ Similar calculations were reported by Smith & Lambert (1987) for mild s -processing ($\tau \leq 0.08 \text{ mb}^{-1}$). A network from Ne to Cu was considered. It was noted that Sc and Co are enriched in such processed material.

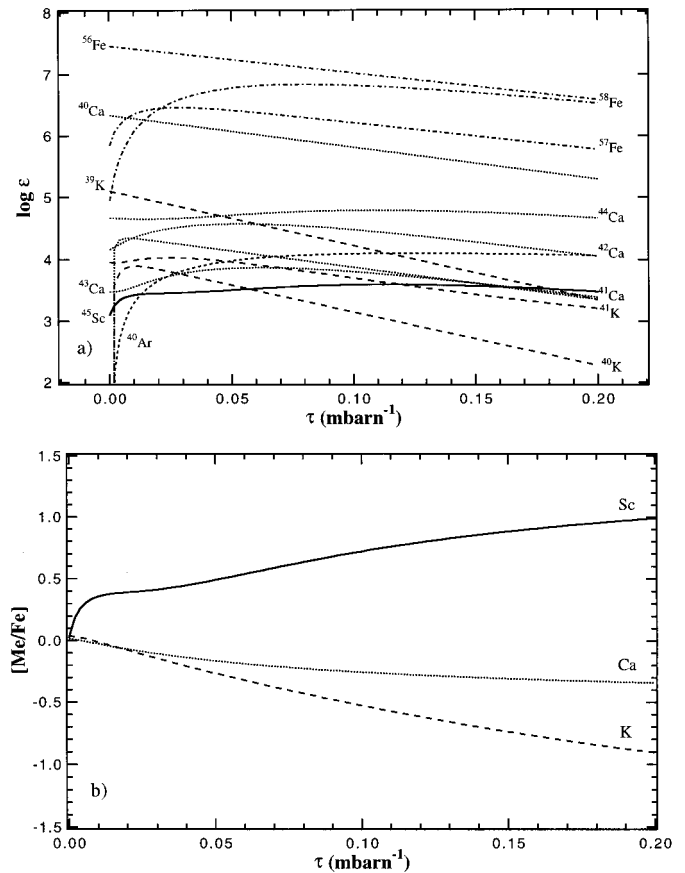


FIG. 13.—Abundances of several light element isotopes (plus iron) as a function of neutron exposure are shown in (a). The initial abundances of ^{40}Ar , ^{40}K , and ^{41}Ca were set to zero; other isotopes were set to the solar abundances. The elemental abundances, as $[\text{Me}/\text{Fe}]$, are shown in (b). The Ar, K, Ca, Sc, and Fe isotopes are indicated by short-dashed, dashed, dotted, solid, and dash-dotted lines, respectively.

neutron density in low-mass stars is $< 10^7 \text{ cm}^{-3}$ for the ^{13}C neutron source.

If the true value of $[\text{Sc}/\text{Fe}]$ in FG Sge is between 0.5 and 1.7 (values estimated by Kipper & Kipper 1993 and by us, respectively), then our calculations show that τ values of at least $\sim 0.05 \text{ mb}^{-1}$ are required. We note that for larger neutron exposures the potassium abundance probably does not decrease as rapidly as indicated by our calculations, since the neutron captures on the lighter species might eventually start feeding into the potassium isotopes. However, this does not lead to significant error for small neutron exposures, given that the lighter isotopes have smaller neutron capture cross sections. As shown in the previous section, the rare earth abundances are well described by a single neutron exposure of about 0.3 mb^{-1} . According to our calculations, such a neutron exposure yields a value of $[\text{Sc}/\text{Fe}]$ near 1.1, and the value of $[\text{Ca}/\text{Fe}]$ has a minimum value of -0.4 near $\tau = 0.4$.

In summary, there exists evidence that the scandium abundance is anomalously high in the atmospheres of some high-luminosity stars including FG Sge. We propose that the scandium abundance in the s -processing region of FG Sge can be increased as a result of a small to moderate strength single neutron exposure. The present surface abundances can be accounted for by extensive mixing with the deep interior such that the surface now consists of a substantial quantity of processed material.

4.2. Is FG Sge a Newborn R CrB Star?

Wallerstein (1990), noting the low-amplitude brightness variations observed in FG Sge, was the first to suggest a link between FG Sge and R CrB stars. Jurcsik (1993) later noted the similarities between the 1992 brightness decline of FG Sge and the R CrB phenomenon. In light of our extensive spectroscopic survey, it is appropriate to examine afresh the question “Is FG Sge now a R CrB star?”

Three observable characteristics define an R CrB star:

1. Deep declines from maximum light occur at irregular intervals.
2. Hydrogen deficiency is indicated from inspection of the spectrum.
3. Enhanced absorption lines of carbon (relative to normal stars of similar atmospheric parameters) are evident. These lines may be from the neutral C atom or the C₂ molecule.

Our contention is that FG Sge exhibits these three characteristics and, hence, deserves the appellation suggested first by Wallerstein (1990) despite certain spectroscopic and photometric differences between it and a “typical” R CrB such as the eponym. We examine first the photometric characteristics and then comment on spectroscopic issues.

The initial deep decline in 1992 marked FG Sge’s photometric transformation to a R CrB star. In particular, there is a close resemblance between FG Sge and V854 Cen: frequent deep declines such that the star is often considerably fainter than maximum light. It is likely not a coincidence that the two stars are similar in other respects (see below). Figure 1 gives the impression that onset of FG Sge’s deep declines may be predictable. Predictability is seemingly at variance with the photometric definition of the R CrB class. There are, however, observational suggestions that the onset of a R CrB’s deep decline occurs at the same pulsational phase for some stars—see Pugach (1977) for RY Sgr and Lawson et al. (1992) for V854 Cen. FG Sge seems at present to exhibit a very similar behavior: deep declines commence at approximately the same pulsation phase each time but a cycle passage may occur without the onset of a deep decline.

As with the photometric changes that occurred recently, evidence on the hydrogen abundance suggests that FG Sge must be a recent convert to the R CrB class. HB report an abundance analysis based on photographic spectra from the 1960s. Relative to Deneb, HB gave the H content up 0.4 dex and He up by an uncertain 0.2 dex, i.e., FG Sge was apparently *less* He rich than Deneb. Langer et al. (1974) found the width of H α to be consistent with the spectral type or T_{eff} derived from spectral scans and excitation temperatures derived from atomic absorption lines, which suggests a near-normal abundance of hydrogen. A key question is “Has FG Sge developed a hydrogen deficiency in the last 20–30 yr?”

One indicator of the H abundance is the strength of the Balmer lines. Our earliest spectrum containing the H α profile, 1992 September, is probably a better indicator of the H abundance than our more recent spectra, because FG Sge had not yet displayed “chromospheric” emission at that time, which might distort the profile. Upon comparing the 1992 September and 1993 August spectra, we find some slight differences between the H α profiles. We have subtracted the (weak) extended nebular emission from the 1992 September spectrum; the resultant H α profile is shown in

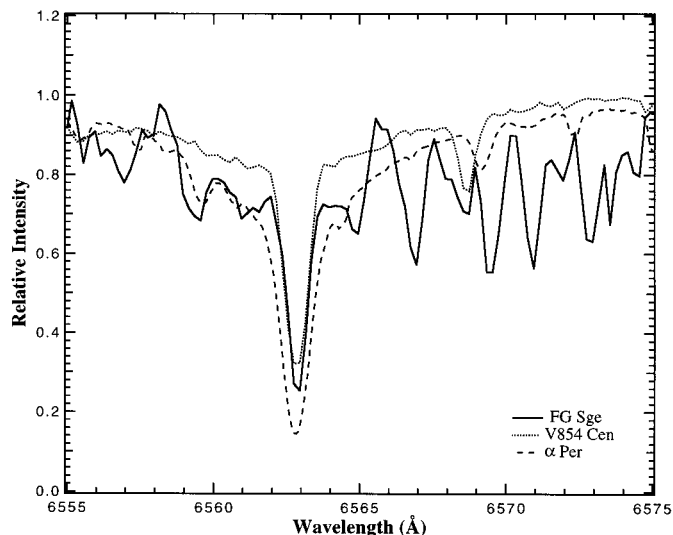


FIG. 14.—H α regions of FG Sge (1992 September), V854 Cen, and α Per. The (weak) nebular emission has been subtracted from spectrum of FG Sge. The spectral resolutions have been matched.

Figure 14. Compared to the H α line of α Per, which has a similar temperature and surface gravity (Gonzalez & Lambert 1996), the H α line on this spectrum of FG Sge has a narrower core and much weaker wings.⁹

The majority of the R CrB stars are severely deficient in hydrogen (down to $\sim 10^{-8}$; Lambert et al. 1998). Certainly, FG Sge does not belong (yet!) with these stars. There is a subset that shows quite strong Balmer lines but a significant hydrogen deficiency nonetheless. Examples are the hot star DY Cen with a H deficiency of slightly more than 1 dex (Jeffery & Heber 1993) and the cooler star V854 Cen with strong Balmer lines (Lawson & Cottrell 1989) that translate to a hydrogen deficiency of 2–3 dex (Asplund et al. 1997b). The H α profile of V854 Cen, which we also show in Figure 14, is a fair match to FG Sge’s profile. Detailed analysis of the Balmer profiles will be required to see if FG Sge now belongs with the rather mildly hydrogen-deficient R CrB stars.

By the third criterion—the presence of carbon features in the spectrum—FG Sge is surely a R CrB star. Strong bands of the C₂ molecule are, as noted previously, evident in our spectra.

Measured against the three defining observational characteristics, FG Sge is probably now a R CrB star. A more detailed comparison of photometric and spectroscopic properties reveals similarities and dissimilarities (Fig. 15), but such close scrutiny is possibly not helpful in answering the question “Is FG Sge a R CrB star?” for the simple reason that at close inspection the known R CrB stars do not form a homogeneous class as observed at maximum or minimum light. By chemical composition, the stars fall into two classes labelled a “majority” and a “minority” group by Lambert & Rao (1994). Members of the former group, comprising R CrB and most other warm R CrB stars, have similar compositions except for a few elements, including

⁹ Another sign of H-deficiency is the relative strength of the CH and C₂ bands. The carbon abundance we derive from the C₂ bands is significantly greater than that obtained from the CH bands (§ 3.2.2). This implies H-deficiency, since to first order CH formation depends on the H abundance but C₂ does not.

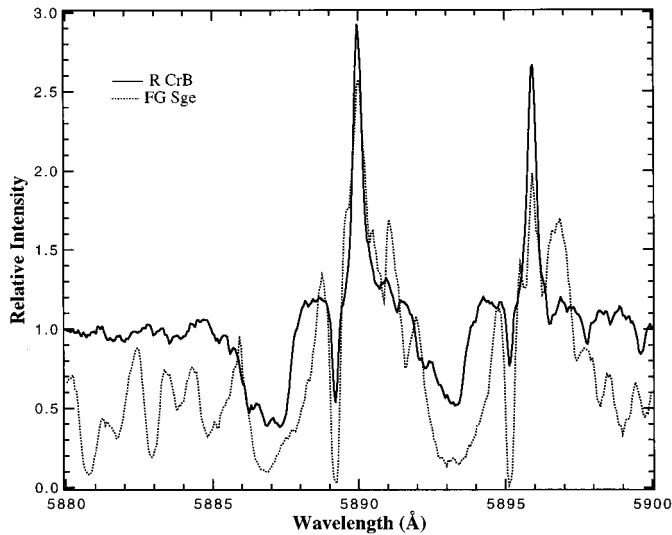


FIG. 15.—Na I D lines of FG Sge on 1994 August 16 compared to same region in R CrB on 1996 May 9. At this time R CrB was recovering from the brightness decline that began in 1995 October, and FG Sge was recovering from the brightness minimum of 1994 May. Both spectra were obtained with the same instrument with similar spectral resolution.

hydrogen. The members of the diverse minority group have several remarkable abundance anomalies. Too little is known at present to place FG Sge in either the majority or the minority group. In addition, Asplund et al. (1997b) note that V854 Cen, which resembles FG Sge photometrically and in hydrogen abundance, has both majority and minority characteristics. They liken V854 Cen to Sakurai's object (Duerbeck & Benetti 1996; Asplund et al. 1997a), which is thought to be a final-flash object. This parallel recalls early suggestions that FG Sge was such an object (see below). We agree tentatively with Jurcsik (1993) that FG Sge is a newborn R CrB star—or at least is temporarily experiencing R CrB-like behavior.¹⁰ In the next section, we discuss physical mechanisms that might account for the photometric and spectroscopic changes seen in FG Sge since 1992 and in R CrB stars.

4.3. Dust Formation Models

Clayton (1996) reviews models proposed to explain the sudden, deep brightness declines of R CrB stars. The most popular ones involve the formation of dust around an R CrB star from material lost from it (originally proposed by O'Keefe 1939; Loreta 1934). The models differ primarily in the location of dust formation with respect to the regions responsible for the narrow and broad emission lines.

Our observations of FG Sge appear to be most consistent with the model proposed by Payne-Gaposchkin (1963) for

¹⁰ The assignment of a variable star to a specific class is an inherently uncertain procedure. In so doing, it is a good idea to keep in mind W. W. Morgan's concept of "morphological groups." A star may belong to a certain morphological group according to its light curve (as with the sudden dips in the light curve of FG Sge that place it in the R CrB group) but not according to its spectrum (*s*-process enhancement much greater than is seen in R CrB stars). What is important is a star's physical properties, not the nomenclature that is used for the category into which an author places the star.

R CrB, whereby dust forms near the photosphere beneath a "chromosphere" and is accelerated by radiation pressure. As the dust layer expands it drags some gas with it, which is expelled from the system. The spectra obtained during the deep minima (especially Fig. 6) strongly imply that the region responsible for the emission lines is in close proximity to the star because (1) the velocity of the emission lines is the same as the absorption-line spectrum observed outside the minima, and (2) the line profile shapes of the inverted emission spectrum are similar to the absorption lines (but more narrow). The emission-line region is probably coincident with the gas responsible for producing the absorption-line spectrum during the out-of-minima epochs. This geometry implies that the dust forms deep in the stellar atmosphere.

The simultaneity of the 1992 deep visual brightness decline of FG Sge and its infrared brightening combined with the regularity of subsequent deep brightness declines (Fig. 1) implies a causal relationship between pulsations and dust formation. The link might be provided by shocks travelling through the atmosphere of FG Sge. The density enhancement in the region behind a shock might lead to dust formation (additional details and relevant references about the dust-shock link can be found in Clayton 1996). However, we do not see evidence of shocks (line-doubling, strong H α emission, or He I emission) in the atmosphere of FG Sge. Among the R CrB stars, only RY Sgr displays clear evidence of shocks, although strong differential atmospheric motions have been noted in R CrB (Rao & Lambert 1997). These facts do not exclude the possibility of shocks altogether, just strong ones.

We note that the 1992 decline of FG Sge is the very first one seen for this star, so it might not be completely appropriate to compare it to R CrB stars; repeated declines in a R CrB star likely result in an extended chromosphere as the gas that fails to reach escape velocity during a mass-loss episode slowly falls back onto the star. Since FG Sge underwent only small-amplitude pulsations prior to the 1992 decline, it probably did not have such an extended chromosphere at that time as the R CrB stars. The lack of chromospheric emission lines in our 1992 September spectrum and Stone, Kraft, & Prosser's (1993) 1992 October, November, and December spectra indicates that FG Sge did not have an extended chromosphere prior to or during the 1992 decline. However, we have certainly seen chromospheric emission lines during the subsequent deep declines.

The chemistry of dust production in R CrB stars has been discussed by Goeres (1993, 1996), Woitke, Krueger, & Sedlmayr (1996b), and Woitke, Goeres, & Sedlmayr (1996a). Cooling of gas by polar molecules triggers carbon nucleation. A leading coolant is carbon monoxide (CO). Detection of CO in or close to the stellar photosphere would be an important diagnostic of dust production. Searches for CO in R CrB stars have proved unsuccessful (Clayton 1996). In this regard, Hinkle, Joyce, & Smith's (1995) observations of CO absorption lines in the 2.3 μm spectrum of FG Sge are of crucial importance.

These observations of first-overtone vibration-rotation CO lines were made about 3 months (one pulsation period) prior to the first large decline. CO was detected at radial velocities of 21 and 43 km s^{-1} . The latter corresponds to our measured photospheric velocity (Table 1). Hinkle et al. derived an excitation temperature (≤ 1800 K) for this component. Thus, FG Sge showed in 1992 evidence of cool gas

at the stellar velocity that may have been close to the photosphere and probably reveals a region with a kinetic temperature sufficiently low for carbon nucleation to occur given a minor perturbation such as might be transmitted up from the pulsating atmosphere. Hinkle et al. estimate the column density of the 43 km s^{-1} CO to about 10^{20} cm^{-2} . If we assume the CO to reside in a layer of thickness 1 stellar radius (about $50 R_{\odot}$), the CO density is about 10^7 – 10^8 cm^{-3} . If the atmosphere is H deficient, He is most likely the major constituent with a density of 10^8 – 10^9 cm^{-3} . These are values of temperature and gas density conducive to dust nucleation in H-deficient atmospheres (Goeres 1996; Woitke et al. 1996a). In short, the CO observations obtained within a pulsational cycle of the first deep decline for FG Sge provide a novel vital clue to dust formation in an H-poor C-rich environment.

4.4. Evolutionary Status

Rapid evolutionary changes accompanied by surface *s*-process and carbon enrichments (products of nucleosynthesis in a He-burning shell) have led to identification of FG Sge as a post-AGB that has (is!) experiencing a final He-shell flash that began about 100 yr ago (Paczyński 1971; Langer et al. 1974; Schönberner 1979; Iben 1984). Iben et al. (1983) and Iben (1984) identify two scenarios that incorporate a He-shell flash (thermal pulse) and restoration of a hot star to the status of a cooler supergiant. Blöcker & Schönberner (1997) dub the scenarios as the “late” pulse and the “very late” pulse:

“*Late*” pulse.—This pulse is initiated in the hot post-AGB star. The star rapidly evolves back to lower effective temperatures, but little mixing between interior and surface is predicted. In particular, dredge-up from the He shell is not expected, and, therefore, the surface should not be enriched in *s*-process products and carbon. A slight enrichment of helium is expected after the star has evolved to $T_{\text{eff}} \leq 7000 \text{ K}$. FG Sge’s trademark—the sudden appearance of *s*-process products in large quantities—cannot be attributed simply to the thermal pulse (Blöcker & Schönberner 1997).

“*Very late*” pulse.—In this case, the post-AGB star is on the white dwarf cooling track before the thermal pulse occurs. Extensive mixing is predicted with drastic reductions of the surface hydrogen abundance and enhancement of carbon and *s*-process products. Detailed calculations for a $0.6 M_{\odot}$ model show the conversion of a normal star to a R CrB-like star (Iben & MacDonald 1995; the *s*-process was not considered in these calculations, but Iben & Livio 1993 argue that it is highly likely that the products would be created and mixed to the surface.)

Evidence from the chemical composition does not yet indicate clearly which, if either, of the two scenarios is to be preferred. The “very late” pulse accounts for the remarkable and recent *s*-process enrichment and the associated carbon enrichment. It predicts a hydrogen deficiency which, as we argue, may be present to a modest degree. The “late” pulse is preferred by Blöcker & Schönberner largely on the grounds that “FG Sge is *not* [their italics] a hydrogen-deficient star.” Additional supporting evidence involves the expansion age of FG Sge’s planetary nebula and the evolutionary timescale. To account for the *s*-process enrichments, Blöcker & Schönberner suppose that this enrichment

occurred in the AGB star but that the *surface* was largely depleted of *s*-process products (and other elements) as the star evolved off the AGB to the white dwarf cooling track. They attribute this depletion to the dust-gas separation held responsible for the very metal poor post-AGB stars (Bond 1991) and field RV Tauri stars (Giridhar, Rao, & Lambert 1994; Gonzalez, Lambert, & Giridhar 1997a, 1997b). Mixing following the thermal pulse homogenizes the thin surface layers of peculiar composition with deeper material having the AGB progenitor’s composition: the anomalous composition created by dust-gas separation is erased and replaced as the surface is enriched quickly in *s*-process products. This ingenious adaptation of the “late” pulse scenario is, however, not readily reconciled with the abundance analysis by HB based on spectra taken in the 1960s before the *s*-process enrichment occurred: 17 elements from C to Eu have the same relative abundances as in Deneb to within approximately ± 0.3 dex. More specifically, elements that condense readily into grains and are grossly underabundant in stars affected by the dust-gas separation process have their normal abundance.

If we use HB’s distance and reddening estimates for FG Sge and apply a bolometric correction, we estimate that in 1970 $\log(L/L_{\odot})$ was about 3.7. Applying post-AGB theoretical evolutionary tracks to FG Sge’s evolution during the last century, Blöcker & Schönberner (1997) estimate that the mass of FG Sge is $0.61 \pm 0.04 M_{\odot}$. Combining these parameters with the temperature estimate of Langer et al. (1974), we calculate that $\log g$ was about 0.90 in ~ 1970 . Assuming the luminosity has remained constant since then and adopting $T_{\text{eff}} \sim 6500 \text{ K}$, the predicted value of $\log g$ is 0.77. This surface gravity estimate can be increased by ~ 0.3 dex if the luminosity is decreased by the same amount, which is within the uncertainty of the distance modulus estimate. This is still significantly smaller than our estimate and that of Montesinos et al. (1990). Strömgren, Olsen, & Gustafsson (1982) note that a helium-rich model atmosphere will have the same effect on the spectrum as a helium-normal atmosphere with a higher gravity. Hence, if FG Sge really is H deficient, then our use of H-normal model atmospheres results in an overestimate of the surface gravity. We plan to test this hypothesis in a future study using H-deficient model atmospheres, where we should be able to derive a physically meaningful surface gravity, which we can then use to constrain evolutionary models.

On balance, the “very late” pulse scenario seems to account better for FG Sge, but it would be desirable to make a careful analysis of the Balmer lines to establish the hydrogen abundance.

5. CONCLUSIONS

FG Sge continues to surprise its admirers. The deep brightness fadings starting in mid-1992 have been accompanied by similarly impressive spectroscopic changes. The C_2 band heads have varied greatly in strength, sometimes disappearing and even appearing in emission during the deep minima. A broad, blueshifted absorption component of each Na I D line appeared after the 1992 decline and gradually broadened, and its velocity increased relative to the photosphere, achieving escape velocity. This, along with increased infrared emission, is evidence of episodic mass loss. The variations in the C_2 band head strengths can be accounted for by variations in T_{eff} consistent with our analysis of the atomic lines. The spectroscopic phenomena

observed during the deep minima, including the C_2 molecular emission, are consistent with an eclipse-type model proposed for R CrB stars, whereby the photosphere is obscured by an ejected dust cloud, which forms near the star but fails to cover the extended chromosphere. As has been shown by Arkhipova, the timing of the deep fades appears to be linked to the quasi-periodic pulsations in the photosphere of FG Sge. The fades begin near maximum light, which correspond roughly with the maximum value of T_{eff} , and reach minimum light in about half a pulsation cycle.

The abundances of carbon, scandium, and the rare earths all appear to be enhanced relative to the Sun and relative to the estimates of Langer et al. We also find evidence that its atmosphere is H deficient by 2–3 dex. These results can be explained in terms of a dredge-up scenario, whereby material from the ^{13}C -rich pocket, which undergoes s-processing with $^{13}\text{C}(\alpha, n)^{16}\text{O}$ as the neutron source, is mixed with the surface layers. A “very late pulse” is the theoretical candidate that seems preferred. Detailed studies of the “late” and “very late” pulse scenarios remain a serious challenge for theoreticians. We note that evolutionary speculations based on the changing pulsation period of FG Sge will need to be modified if it turns out that its atmosphere is significantly H deficient. It might even be possible to determine the timing of the helium dredge-up episode from a

careful study of the evolution of the pulsation period and amplitude since 1970.

We propose another challenge—this one for laboratory spectroscopists. One fact made painfully clear in our syntheses of the spectrum of FG Sge is the lack of adequate atomic data for the rare earth elements. Of course, we also encourage continued monitoring of FG Sge, especially with infrared photometry.

We thank B. Carney for obtaining a spectrum of FG Sge at our request. We also thank C. Sneden for his abundance analysis program, R. Kurucz for his model atmospheres, F. Käppeler for helpful advice concerning neutron capture cross sections, and M. Asplund for helpful advice on H-deficient atmospheres. We have used, and acknowledge with thanks, photometric data from the AAVSO, AFOEV, BAAVSS, and VSOLJ databases; the importance of these observations to our study cannot be overemphasized. We have also made use of the SIMBAD database, operated at CDS, Strasbourg, France. This research has been supported in part by the National Science Foundation (grants AST-9315124 and AST-9618414), the Robert A. Welch Foundation of Houston, Texas, and the Kennilworth Fund of the New York Community Trust.

REFERENCES

- Acker, A., Jасhek, M., & Gleizes, F. 1982, *A&AS*, 48, 363
 Anders, E., & Grevesse, N. 1989, *Geochim. Cosmochim. Acta*, 53, 197
 Arkhipova, V. P. 1994, *Pis'ma Astron. Zh.*, 20, 919
 ———. 1996, *Pis'ma Astron. Zh.*, 22, 828
 Asplund, M., Gustafsson, B., Lambert, D. L., & Rao, N. K. 1997a, *A&A*, 321, L17
 Asplund, M., Gustafsson, B., Rao, N. K., & Lambert, D. L. 1997b, in preparation
 Beer, H., Voss, F., & Winters, R. R. 1992, *ApJS*, 80, 403
 Blöcker, T., & Schönberner, D. 1997, *A&A*, in press
 Bond, H. E. 1991, in *Evolution of Stars: the Photospheric Abundance Connection*, ed. G. Michaud & A. V. Tutukov (Dordrecht: Kluwer), 341
 Clayton, D. D. 1983, *Principles of Stellar Evolution and Nucleosynthesis* (Chicago: Univ. of Chicago Press)
 Clayton, D. D., & Rassbach, M. E. 1967, *ApJ*, 148, 69
 Clayton, G. C. 1996, *PASP*, 108, 225
 Cohen, R. D., Marcy, G. W., & Harlan, E. A. 1980, *AJ*, 85, 867
 Corliss, C. H., & Bozman, W. R. 1962, *Experimental Transition Probabilities for Spectral Lines of Seventy Elements* (NBS Monograph 53) (Washington, DC: US Government Printing Office)
 Cowley, C. R., Jасhek, M., & Acker, A. 1985, *A&A*, 149, 224
 Duerbeck, H. W., & Benetti, S. 1996, *ApJ*, 468, L111
 Faulkner, W., & Bessell, M. S. 1970, *PASP*, 82, 1333
 Flannery, B. P., & Herbig, G. H. 1973, *ApJ*, 183, 491
 Gallino, R., Arlandini, C., Busso, M., Lugaro, M., Travaglio, C., Straniero, O., Chieffi, A., & Limongi, M. 1997, *ApJ*, submitted
 Giridhar, S., Rao, N. K., & Lambert, D. L. 1994, *ApJ*, 437, 476
 Goeres, A. 1993, *Rev. Mod. Astr.*, 6, 165
 ———. 1996, in *ASP Conf. Proc. 96, Hydrogen-deficient Stars*, ed. C. S. Jeffery & U. Heber (San Francisco: ASP), 69
 Gonzalez, G., & Lambert, D. L. 1996, *AJ*, 111, 424
 Gonzalez, G., Lambert, D. L., & Giridhar, S. 1997a, *ApJ*, 479, 427
 ———. 1997b, *ApJ*, 481, 452
 Harrington, J. P., & Marionni, P. A. 1976, *ApJ*, 206, 458
 Herbig, G. H., & Boyarchuk, A. A. 1968, *ApJ*, 153, 397
 Hinkle, K. H., Joyce, R. R., & Smith, V. V. 1995, *AJ*, 109, 808
 Iben, I., Jr. 1984, *ApJ*, 277, 333
 Iben, I., Jr., Kaler, J. B., Truran, J. W., & Renzini, A. 1983, *ApJ*, 264, 605
 Iben, I., Jr., & Livio, M. 1993, *ApJ*, 406, L15
 Iben, I., Jr., & MacDonald, J. 1995, in *White Dwarfs*, ed. D. Koester & K. Werner (Berlin: Springer), 48
 Iijima, T. 1996, *MNRAS*, 283, 141
 Iijima, T., & Strafella, F. 1993, *Inf. Bull. Variable Stars*, 3959
 Jeffery, C. S., & Heber, U. 1993, *A&A*, 270, 167
 Jurcsik, J. 1993, *A&A*, 43, 353
 Kipper, T. 1996, in *ASP Conf. Proc. 96, Hydrogen-deficient Stars*, ed. C. S. Jeffery & U. Heber (San Francisco: ASP), 329
 Kipper, T., & Kipper, M. 1989, in *IAU Colloq. 106, Evolution of Peculiar Red Giants*, ed. H. R. Johnson & B. Zuckerman (Cambridge: Cambridge Univ. Press), 146
 ———. 1993, *A&A*, 276, 389
 Kipper, T., Kipper, M., & Klochkova, G. 1995, *A&A*, 297, L33
 Kurucz, R. L. 1979, *ApJS*, 40, 1
 ———. 1989, updated version of Kurucz & Peytremann line list provided on magnetic tape
 ———. 1993, *ATLAS 9 Stellar Atmosphere Programs and 2 km/s Grid* (CD-ROM Vol. 13) (Cambridge: Smithsonian Astrophysical Observatory)
 Kurucz, R. L., & Peytremann, E. 1975, *A Table of Semiempirical g_f -Values* (SAO Special Rep. 362) (Cambridge, MA: Smithsonian Astrophysical Observatory)
 Lambert, D. L., & Rao, N. K. 1994, *J. Ap. Astr.*, 15, 47
 Lambert, D. L., Rao, N. K., Gustafsson, B., & Asplund, M. 1998, in preparation
 Langer, G., Kraft, R. P., & Anderson, K. S. 1974, *ApJ*, 189, 509
 Lawson, W. A., & Cottrell, P. L. 1989, *MNRAS*, 240, 689
 Lawson, W. A., Cottrell, P. L., & Clark, M. 1991, *MNRAS*, 251, 687
 Lawson, W. A., Cottrell, P. L., Gilmore, A. C., & Kilmartin, P. M. 1992, *MNRAS*, 256, 339
 Loreta, E. 1934, *Astr. Nach.*, 254, 151
 Malaney, R. A. 1987a, *Ap&SS*, 137, 251
 ———. 1987b, *ApJ*, 321, 832
 McCarthy, J. K., Sandiford, B. A., Boyd, D., & Booth, J. 1993, *PASP*, 105, 881
 Montesinos, B., Cassatella, A., Gonzalez-Riestra, R., Fernandez-Castro, T., Eiroa, C., & Jimenez-Fuensalida, J. 1990, *ApJ*, 363, 245
 Moore, C. E., Minnaert, M. G. J., & Houtgast, J. 1966, *The Solar Spectrum 2935 Å to 8770 Å* (NBS Monograph 61) (Washington, DC: NBS)
 O'Keefe, J. A. 1939, *ApJ*, 90, 294
 Paczyński, B. 1971, *Acta Astron.*, 21, 417
 Payne-Gaposchkin, C. 1963, *ApJ*, 138, 320
 Pugh, A. F. 1977, *Inf. Bull. Variable Stars*, 1277
 Rao, N. K., & Lambert, D. L. 1997, *MNRAS*, 284, 489
 Reddy, B. E., Parthasarathy, M., Gonzalez, G., & Bakker, E. J. 1997, *A&A*, in press
 Renzini, A. 1990, in *ASP Conf. Proc. 11, Confrontation between Stellar Pulsation and Evolution*, ed. C. Cacciari & G. Clementini (San Francisco: ASP), 549
 Schönberner, D. 1979, *A&A*, 79, 108
 Smith, V. V., & Lambert, D. L. 1987, *MNRAS*, 227, 563
 Smolinski, J., Climenhaga, J. L., & Kipper, T. 1976, *PASP*, 88, 67
 Sneden, C. 1973, Ph.D. thesis, Univ. of Texas at Austin
 Stone, R. P. S., Kraft, R. P., & Prosser, C. F. 1993, *PASP*, 105, 755
 Strömgren, B., Olsen, E. H., & Gustafsson, B. 1982, *PASP*, 94, 5

- Takens, R. J. 1970, *A&A*, 5, 244
Ulrich, R. K. 1973, in *Explosive Nucleosynthesis*, ed. D. N. Schramm & Arnett, W. D. (Austin: Univ. Texas Press), 139
van Genderen, A. M. 1994, *A&A*, 284, 465
van Genderen, A. M., & Gatschy, A. 1995, *A&A*, 294, 453
Vanture, A. D., Wallerstein, G., Brown, J. A., & Bazan, G. 1991, *ApJ*, 381, 278
Vogt, S. S., et al. 1994, *Proc. SPIE*, 2198, 362
Wagemans, C., Druyts, S., & Barthélemy, R. 1995, in *Nuclei in the Cosmos III*, ed. M. Busso, R. Gallino, & C. M. Raiteri (New York: AIP), 169
Wallerstein, G. 1990, *ApJS*, 74, 755
Wentzel, W., & Fürtig, W. 1967, *Sterne*, 43, 19
Wheeler, J. C., Sneden, C., & Truran, J. W., Jr. 1989, *AR&A*, 27, 279
Woitke, P., Goeres, A., & Sedlmayr, E. 1996a, *A&A*, 313, 217
Woitke, P., Krueger, D., & Sedlmayr, E. 1996b, *A&A*, 311, 927
Woodward, C. E., Lawrence, G. F., Gehrz, R. D., Jones, T. J., Kobulnicky, H. A., Cole, J., Hodge, T., & Thronson, H. A., Jr. 1993, *ApJ*, 408, L37
Woosley, S. E., Fowler, W. A., Holmes, J. A., & Zimmerman, B. A. 1978, *Atomic Data Nucl. Data Tables*, 22, 371